

2024

Hesselø South Offshore Wind Farm Geoarchaeological Analysis

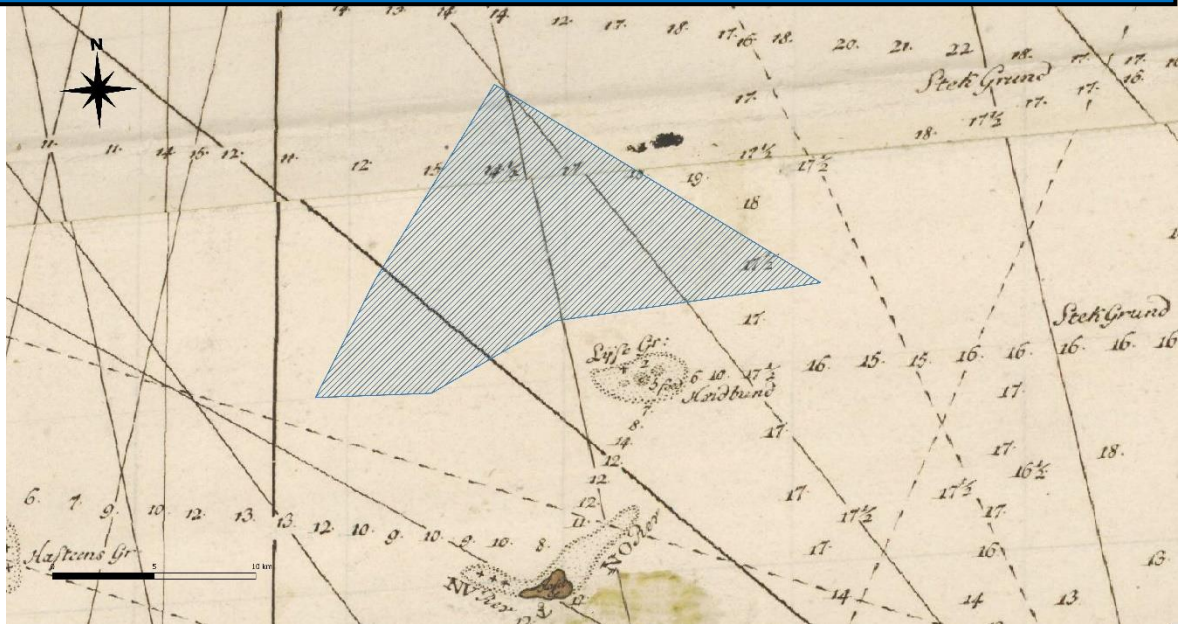


Figure 1. The planned project area for Hesselø South Offshore Wind Farm projected on a sea chart from 1773.

Moesgaard Museum

18-09-2024

Revision B

Contents

1 Resume (dansk)	2
1.1 Abstract.....	3
1.2 List of abbreviations.....	4
1.3 List of figures.....	5
2 Introduction	7
2.1 Project background.....	7
2.2 Administrative and other data.....	8
2.3 Project goals.....	9
2.4 Scope of work.....	10
2.4.1 Deviations from Scope of work	10
2.5 Reference documents.....	10
3 Submerged Stone Age potential	11
3.1 Preservation	13
3.2 Knowledge lacunae	13
3.1 Geological development in the Hesselø area	15
3.1.1 Pre-Quaternary geology	15
3.1.2 Late Glacial and Holocene geology	15
3.3 Borehole data.....	16
4 Modelling sea levels.....	16
4.1 Collection of data	16
4.2 Modelling sea levels – creating a shoreline displacement curve	20
4.3 Sub-bottom seismology and landscape correction	24
4.4 Coastline Models.....	26
4.5 Areas of archaeological interest	32
5 Cultural historical archaeology	32
5.1 Methods	32

5.2 Results	34
5.2.1 SSS-anomalies	35
5.2.2 MAG-anomalies	36
6 Conclusions	38
Literature:	38
Appendices:	40
Appendix 8.0 ARCHAEOLOGY CONFIDENCE 1 SSS-anomalies	40
Appendix 8.1 ARCHAEOLOGY CONFIDENCE 2 SSS-anomalies	41
Appendix 8.2 ARCHAEOLOGY CONFIDENCE 3 SSS-anomalies	43
Appendix 8.3 ARCHAEOLOGY CONFIDENCE 4 SSS-anomalies	61
Appendix 8.4 MAG-anomalies	64
Appendix 8.5 Borehole data	76
Appendix 8.6 Contextual information about samples	79

1 Resume (dansk)

Marinarkæologi Vestdanmark (MAV) har udarbejdet nærværende geoarkæologiske analyse for Energinet med henblik på at kortlægge potentielle kulturhistoriske interesser på havbunden for den planlagte havvindmøllepark Hesselø South. Den geoarkæologiske undersøgelse konkluderer at anlægsarbejdet ikke vurderes at være til risiko for fortidsminder fra stenalderen. En arkæologisk forundersøgelse, som har til hensigt at identificere stenalderbosættelser, anbefales derfor ikke.

Rapporten har også til formål at identificere de vrage og rester af skibslaster, der er i området. I analysen er der derfor også blevet udpeget anomalier på baggrund af de af Energinet leverede geofysiske data. Vurderingerne og udpegningerne er mere konkret blevet baseret på side-scan sonar data, magnetometer data, multibeam data og diverse kulturhistoriske registre.

Der er i alt udpeget 310 Side Scan Sonar-anomalier (SSS-anomalier) i projektområdet. Af disse tilskrives 13 CONF 1, 34 CONF 2, 196 CONF 3 og 67 CONF 4 (formentlig moderne MMO'er (man-made objects)). Blandt anomalierne er et muligt anker (HS_B04_SSS_GO6_0707) og 3 anomalier som tolkes som skibsvrage (HS_B02_SSS_GO6_0523, HS_B03_SSS_GO6_0106,

HS_B05_SSS_GO6_0291). MAV anbefaler ROV (remotely operated vehicle) eller dykkerbesigtigelser af CONF 1 og CONF 2 samt mitigation of CONF 3 anomalier af AEZ.

Det er Slots og Kulturstyrelsen (SLKS), der har til opgave at beslutte hvilke af de udpegede anomalier, som skal besigtiges og eventuelt friholdes som et led i en forundersøgelse. Det er ligeledes SLKSs rolle at fastsætte eventuelle friholdelseszoner omkring vrage og anomalier mm. Nærværende rapport kan således betragtes som en museal anbefaling, hvorfra SLKS kan træffe deres afgørelse.

1.1 Abstract

On behalf of Energinet, the Maritime Archaeology of Western Denmark (MAV) has carried out the present desk-based geoarchaeological study of the project area ahead of the construction of the offshore wind farm Hesselø South. The geoarchaeological analysis concludes that the construction work is not considered to be a major risk for prehistoric Stone Age settlements. An archaeological pre-investigation that aims to identify potential Stone Age settlements is therefore not recommended.

In the analysis anomalies have also been identified based on the geophysical data supplied by Energinet. The assessments and designations are based on side-scan sonar data, magnetometer data and multibeam data. There are 310 SSS anomalies detected in the project area. Of these, 13 are designated CONF 1, 34 CONF 2, 196 CONF 3 and 67 CONF 4 (most likely modern MMOs). Among the anomalies is one potential anchor (HS_B04_SSS_GO6_0707) and 3 anomalies interpreted as shipwrecks (HS_B02_SSS_GO6_0523, HS_B03_SSS_GO6_0106, HS_B05_SSS_GO6_0291). MAV recommends the ROV and/or diver investigation of CONF 1 (= 13) and CONF 2 (= 34) anomalies as well as the mitigation of CONF 3 (= 196) anomalies by AEZ.

It is the responsibility of the Ministry of Culture (SLKS) to decide which of the above-mentioned anomalies that should be inspected and possibly protected as part of an archaeological pre-survey. It is also the role of SLKS to define exclusion zones around wrecks and anomalies etc. The following report should therefore be regarded as museum recommendation from which SLKS can make their decision.

1.2 List of abbreviations

AEZ	Archaeological Exclusion Zone
BC	Before Christ
BH	Borehole
BSU	Base Seismic Unit
CE	Current Events
CPT	Cone Penetration Test
DKM	De Kulturhistoriske Museer i Holstebro
EI	Energy Island
EOD	Explosive Ordnance Disposal
FFM	Fund og Fortidsminder
GEUS	De Nationale Geologiske Undersøgelser for Danmark og Grønland
GIS	Geographic Information System
HF	High Frequency
LF	Low Frequency
MAG	Magnetometer
MAJ	Marinarkæologi Jylland
MASL	Meters Above Sea Level
MAV	Marinarkæologi Vestdanmark
MBES	Multibeam Echo Sounder
MMO	Man Made Object
MOMU	Moesgaard Museum
NKM	Nordjyllands Kystmuseum
OWF	Offshore Wind Farm
P2P	Peak to peak
ROV	Remotely Operated Vehicle
SBP	Sub-Bottom Profiler
SLIP	Sea Level Index Point
SLKS	Slots- og Kulturstyrelsen
SOW	Scope Of Work
SSS	Side Scan Sonar
UXO	Unexploded Ordnance
VIR	Vikingskibsmuseet i Roskilde
WWI	World War One
WWII	World War Two

1.3 List of figures

Figure 1. The planned project area for Hesselø South Offshore Wind Farm projected on a sea chart from 1773.....0

Figure 2. New placement of Hesselø OWF compared to the original area Source: Energinet.7

Figure 3. The area of the Hesselø Wind farm with the areas of responsibility for Moesgaard Museum and the Viking Ship Museum marked.....8

Figure 4. Schematic of cultural and natural developments in South Scandinavia in calibrated years BC. (Astrup 2018).12

Figure 5. Borehole positions shown in blue (Numbers refer to ID number in Appendix 8.6. and sea-level curve in Figure. 6 and show dated samples. Cone penetration test (CPT) positions are shown in red.17

Figure 6. Sea-level curve where the dashed line gives the hypothesized sea level in the planned OWF area during the Holocene. Marine samples are shown in blue whereas terrestrial samples are shown in green.22

Figure 7. Sea-level curve from Jensen and Bennike (2020).23

Figure 8. Depositional environment for Unit B including several estuaries, back-barrier basins, bars and spits. Hesselø South area and cable route are marked by a black line. Moreover, the previous Hesselø area and Area B is marked by a red dotted line.26

Figure 9. Modern bathymetry in the Hesselø South OWF area.27

Figure 10. Distance from seabed to H20 in meters. The lowest/deepest areas recognized on H20 are important because they can be thought to represent lake basins that are filled with sediment. The material that is deposited over the archaic lake basins, peat layers, etc. both preserves them and makes them difficult to research. Higher areas on slopes are more exposed and subject to erosion but are also better suited to diver reconnaissance precisely because settlement traces are not buried under a thick layer of sediment. Identification of the areas with the greatest Holocene layer formation shows both 1) where archaeological materials can have avoided erosion, 2) where it would be difficult to access layers using divers, and 3) where layers are too deep to be affected by

construction work. Therefore, archaeological surveys should be planned in the areas best suited for settlement where past sedimentation allows such investigations without extreme difficulty in accessing the layers.28

Figure 11. Coastline position at -15 m below msl corresponding to the time around 7500 cal BC. Drawn according to the lowest postglacial horizon H20. As it can be seen the area was completely transgressed at this time.29

Figure 12. Coastline position at -20 m below msl corresponding to the time around 8400 cal BC. Drawn according to the lowest postglacial horizon H20. As it can be seen the area was completely transgressed at this time.29

Figure 13. Coastline position at -25 m below msl corresponding to the time around 9400 cal BC. Drawn according to the lowest postglacial horizon H20. As can be seen from the model there might have been an exposed land surface in the southwestern corner.30

Figure 14. Coastline position at -30 m below msl. Drawn according to the lowest postglacial horizons H20. It is uncertain if the water level has been as low as modelled.30

Figure 15. Coastline position at -35 m below msl. Drawn according to the lowest postglacial horizons (H20). It is uncertain if the water level has been as low as modelled.31

Figure 17. Map over the SSS-anomalies.36

Figure 18. Map over the MAG-anomalies.....37

Figure 19. The wreck of BORINGIA with the MAG-tracks overlaid on top of the SSS-mosaic.....37

2 Introduction

2.1 Project background

Hesselø Offshore Wind Farm is the second offshore wind farm (OWF) to be built as part of the Energy Agreement of 29th of June 2018. The project was paused during June 2021, however, it has since been discovered during Energinet’s preliminary surveys that the sea bottom was too soft in many parts of the originally proposed project area. On 25 June 2022, the Danish Government and other parties decided that Hesselø offshore wind farm is to be moved to an area south of the original area (Figure 2).

The political agreement on the new position follows a new fine screening conducted by COWI for the Danish Energy Agency. The fine screening was published on 11 May 2022, and it shows that the area south of the original area is a good alternative since the seabed has been assessed as better suited for establishment of the wind farm.

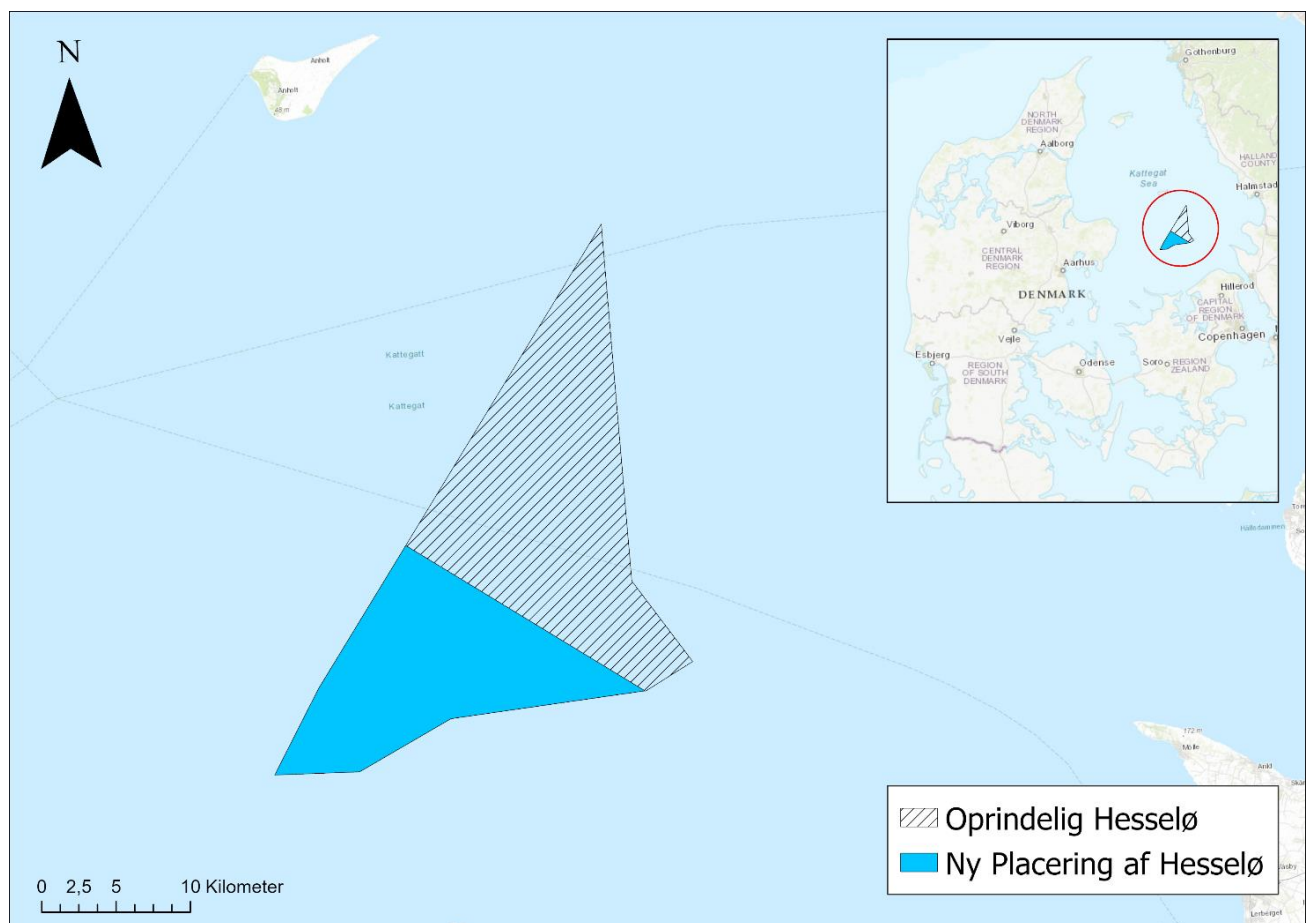


Figure 2. New placement of Hesselø OWF compared to the original area Source: Energinet.

2.2 Administrative and other data

The geoarchaeological analysis is carried out for Energinet. The contact person is Weronika Marta Szelech Søe. Moesgaard Museum (i.e. MAV) is responsible for the archaeology in the OWF area (Figure 3).

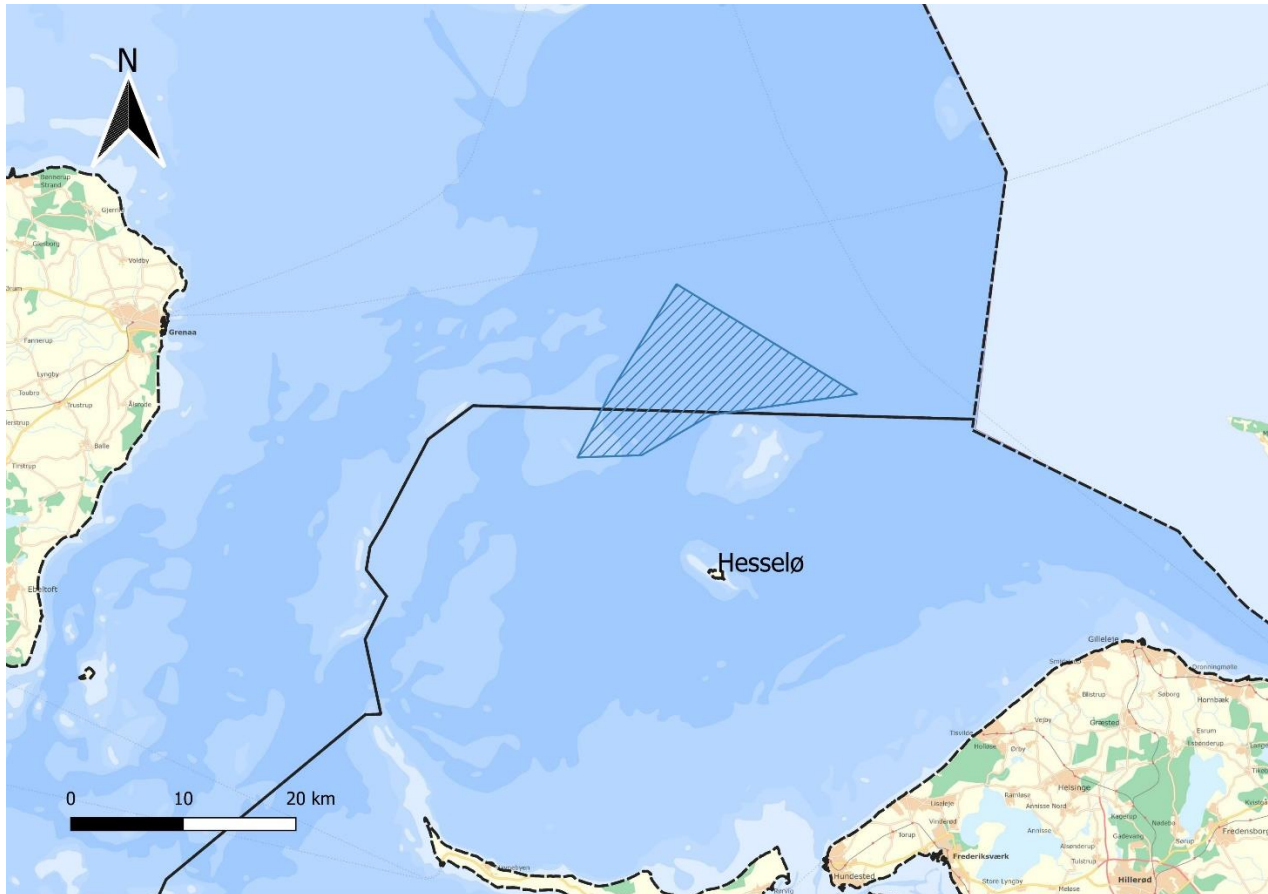


Figure 3. The area of the Hesselø Wind farm with the areas of responsibility for Moesgaard Museum and the Viking Ship Museum marked.

At the MERE HAVVIND 2030 MARINARKÆOLOGI KICK OFF meeting held on the 1st of February 2023 it was decided that the responsibility for the geoarchaeological analysis lies with Moesgaard Museum. The contact people are Daniel Peter Dalicsek (DAD) and Peter Astrup (PMA).

The wind farm operator and company responsible for construction has not been found yet. However, it is advised that the company selected for those tasks in the future contacts MAV as early as possible during the planning process to mitigate questions concerning maritime archaeology. The geoarchaeological analysis is archived at Moesgaard Museum under the filing number MAV2023-050.

Responsible museum:	MAV, VIR
Museum contact:	Daniel Peter Dalicsek
Report responsibility:	Daniel Peter Dalicsek og Peter Moe Astrup
Report due date:	30.08.2024
Archaeologists:	DAD (MOMU), PMA (MOMU)
Stone Age specialist:	PMA (MOMU), KRF (GEOSCIENCE, AU)
Historical archaeology specialist:	DAD (MOMU)
Lokalitetsnavn:	Hesselø South Havvindmøllepark
Systemnr:	249618
Sted- og lok.nr (FF):	400120c-1346 Kattegat V
MAV journal number:	MAV2023-050 Hesselø South
SLKS journal number:	
Budget incl. VAT:	
Dato for confirmed budget:	
Budget type:	Voluntary agreement
Period for analysis:	2023-2024
Client	Energinet
Client address	Tonne Kjærvej 65, 7000 Fredericia
Client type	Public
Client CVR nr.	28980671
Coordinates:	X 664264.8 Y 6250619.2
Coordinate system:	Euref89 UTM zone 32N
Water depth:	19,4-33,0m
Area for analysis:	164,454 km ²

2.3 Project goals

The goal of the geoarchaeological analysis is to analyse, identify, locate, and map wrecks and wreckage on or buried underneath the seafloor, as well as prehistoric landscapes meaning locations of potential archaeological interest such as submerged coastal zones that could have served as

prehistoric settlement sites. Furthermore, the geoarchaeological analyses aims to judge the potential for preservation of possible finds and find locations.

According to best practice the geoarchaeological analysis follows the geological surveys and it is followed by maritime archaeological surveys if deemed necessary in the project chronology.

2.4 Scope of work

The geoarchaeological analysis is conducted in the period December 2023 to August 2024. The deadline for the report is the 30th august 2024. The report covers the entire planned wind farm area and includes all available data and resources.

2.4.1 Deviations from Scope of work

There are no deviations from the scope of work.

2.5 Reference documents

Document	Title	Author
HESSELØ HAVVINDMØLLEPARK KABEL Geoarkæologisk analyse af geofysiske data for planlagt kabeltracé VIR 2932		VIR
HESSELØ HAVVINDMØLLEPARK GEOARKÆOLOGISK ANALYSE FOR MØLLEOMRÅDE MAJ2020-58		MOMU
Bilag 1 – 2023-02-01 MH2030. Marinarkæologi.pdf		ENERGINET
Tidsplan milepæle.xlsx		ENERGINET
ACTION LIST.xlsx		ENERGINET
22/02940-1 Appendix 1 Scope of services incl. Encl1-4.pdf		ENERGINET

DOW2030_POL_HesseloeSouth.zip		ENERGINET
16/03737-3	Best Practice - Marinarkæologi	ENERGINET/SLKS
SCREENING OF SEABED GEOLOGICAL CONDITIONS FOR THE OFFSHORE WIND FARM AREA HESSELØ SOUTH AND THE ADJACENT CABLE CORRIDOR AREA. DESK STUDY FOR ENERGINET.		GEUS,
GEOPHYSICAL SURVEYS FOR DANISH OFFSHORE WIND 2030 – HESSELØ SOUTH.		GEOxyz

3 Submerged Stone Age potential

During the Late Pleistocene a thick layer of ice covered large parts of modern Denmark. Approximately 20,000 years ago the ice began to retreat, partly because of melting due to increasing temperatures and partly because of glaciers calving icebergs into the sea. Enormous quantities of glacial meltwater were released into the world's oceans throughout the Mesolithic period which ended about 6,000 years ago. Studies have shown that global sea levels have risen 130m since the Late Glacial Maximum around 22,000 years ago (Fairbanks 1989; Lambeck et al. 2014). Peat layers described in core logs in the project area are also evidence of sea levels previously being lower than today. Although sea level changes of the Stone Age are still not precisely described in the Hesselø South region, it is clear that any possible preserved Stone Age sites can date to the Late Palaeolithic or Early Mesolithic. The Late Palaeolithic dates to ca. 12,800 – 9,500 BC, while the Mesolithic dates to ca. 9500-4000 BC (see cultural developments in the Mesolithic, Figure 4).

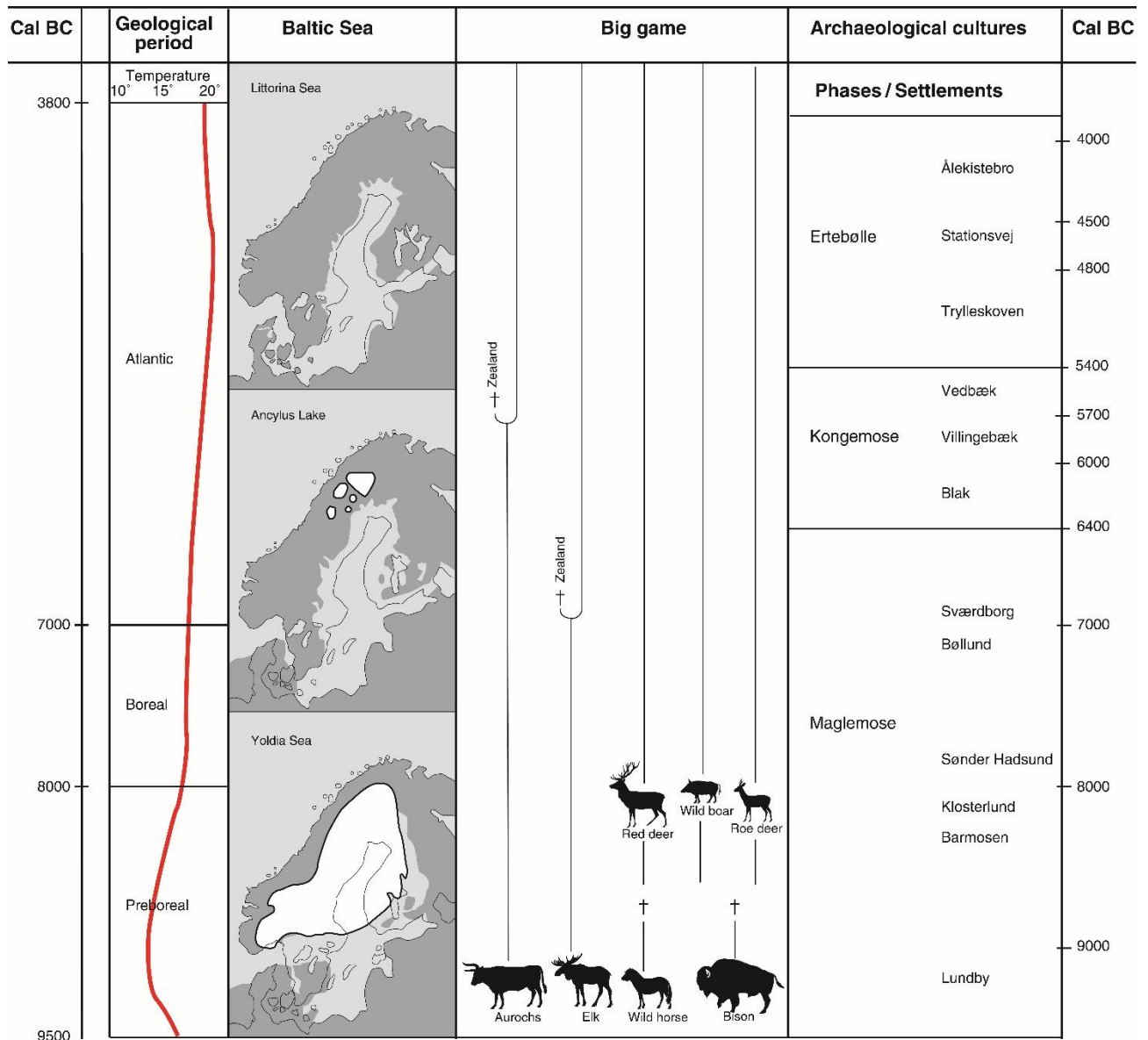


Figure 4. Schematic of cultural and natural developments in South Scandinavia in calibrated years BC. (Astrup 2018).

Many years of archaeological investigations have shown that Stone Age people did not randomly occupy landscapes. Rather, they chose their locations strategically based on a range of parameters in order to secure access to necessary resources, cultivate social networks, and maintain demographic viability. By reconstructing the now submerged landscapes as they appeared at various points in the past, it is possible to pinpoint areas that were better suited than others to obtain the necessary conditions for prehistoric lifestyles. Creating a detailed picture of the prehistoric landscape(s) is therefore vital for understanding where the coming construction work is at its highest risk of destroying potential archaeological localities. Evaluating an area’s potential of having Stone Age

settlements is typically based on topographic variables such as the presence of lakes, streams, and coasts. However, in practice, different periods varied widely in their requirements for specific natural features and their accompanying resources. Most of the source material for our understanding of prehistoric hunter-gatherers in Denmark in the millennia prior to the Neolithic comes from coastal settlements, yet as of this writing it is unclear to what extent Late Palaeolithic and Early Mesolithic people also prioritized these areas.

In the area to be occupied by the Hesselø South OWF, potential Stone Age settlements (coastal as well as inland) are now on (or under) the sea floor – a location that is both difficult and expensive to survey. It is precisely here, however, that the last years of underwater archaeology has shown its potential for making major scientific advances in the Danish inshore waterways. This is primarily due to two factors which can be characterized as “Preservation” and “Knowledge lacunae”:

3.1 Preservation

Conditions of preservation on submerged settlements are renowned for being extremely good for organic materials such as wood and bones (see examples in Andersen 2013). This is the result of continuously rising sea levels that inundated coastal settlements. In the process, the archaeological layers and materials were enclosed in anoxic surroundings which have remained that way to the present day. Because of the special environment in these submerged cultural layers oxygen was not present in sufficient amounts to allow the onset of decay, creating a sort of time capsule. Previous investigations of submerged settlements from the Kongemose and Ertebølle cultures have provided completely new insights into the types of wooden implements used in the Stone Age. This provides the example for the huge scientific potential that submerged and buried Stone Age sites in the Kattegat region could hold.

3.2 Knowledge lacunae

Submerged Stone Age landscapes on the sea floor represent one of the biggest unexplored areas in the Danish archaeological milieu. Therefore, they likely contain information that can fill some gaps in our knowledge which have remained unanswered by archaeological investigations since the various periods of the Stone Age was recognized. It is still unknown, for example, what role coasts played in the early Mesolithic (9500-6400 BC), as the subsistence economy of that period is almost exclusively known from archaeological remains found at inland sites far from them. In order to detect the earliest traces of coastal exploitation in Denmark, Moesgaard Museum has in recent years attempted to locate Maglemose culture sites near or at the archaic coastline which is now submerged

in Aarhus Bay. Aarhus Bay is of special interest because it consists of sheltered waters where potential Maglemose culture settlements occur in water depths that are shallower than in more southern areas of Denmark. In 2017, 23 locations in the bay were tested and one produced dispersed flint flakes and blades at a depth of -8.0 masl. Consequently, a small excavation was conducted two months later to determine whether remains of a coastal settlement was present. This investigation showed that immediately below the seabed there was an in-situ deposit with worked flint (including diagnostic microliths) and organic materials some of which have been ¹⁴C-dated to the latest part of the Maglemose culture (Astrup 2018). The find layer represents a coastal settlement and later investigations have recovered fish bones from the site which demonstrates that exploitation of marine species and coastal fishery took place as early as during the Maglemose period. Targeted diving investigations in archaic coastal areas are therefore a prerequisite for resolving important research questions such as:

- How widespread was coastal settlements in the Late Palaeolithic and Maglemose cultures?
- How important a role did marine resources play in subsistence and what methods were used to collect them?
- Were coastal settlements occupied longer than those inland? Did the same people use both types of sites, or were there some groups who occupied the coast while others remained inland?

The above points serve to illustrate that there is much we still do not know about life along the coasts in the early Mesolithic/Maglemose culture (and particularly in the remote offshore areas). Thus, it is a difficult task to decide where in the landscape people settled. However, this does not change the fact that it is crucial to have as detailed an understanding of the landscape as possible, since it formed the basis of life for the people who lived in the construction area. Considering this, the next section of the report aims to step-by-step recreate a detailed picture of the now submerged cultural landscape in the OWF area. The goal is to be able to evaluate which areas have the greatest potential for prehistoric settlements and whether they will still contain preserved remains today. In concrete terms this means constructing a model of past sea levels and using the geophysical data to identify relevant archaic terrain.

3.1 Geological development in the Hesselø area

3.1.1 Pre-Quaternary geology

The Sorgenfrei-Tornquist fault zone is known as the plate tectonic boundary between the Baltic Shield and Avalonia. The Baltic Shield consists of bedrock and Avalonia consists of sedimentary rocks. The Sorgenfrei-Tornquist zone extends across Skåne in Sweden to Kattegat to North Jutland with a south-east to north-west orientation. The fault zone goes through the Hesselø South area. The bedrock in the Hesselø South OWF consists of Jurassic and Upper Cretaceous sandy mudstone (Erlström et al. 2001).

3.1.2 Late Glacial and Holocene geology

The Hesselø South area is located between Zealand, Djursland, and Sweden. Several glacial events have been documented in the Danish Northern area since the Last Glacial Maximum (LGM) 22,000 years ago when the ice margin reached the Main Stationary line in central Jutland (Houmark-Nielsen et al. 2012). At that time the Hesselø South area was subglacial undergoing associate processes such as formation of subglacial meltwater channels, glaciotectonic movements, and deposition of till. Since the LGM a rising temperature trend has been seen in the global climate. The rising temperature initiated the retreat of ice sheets and together with icebergs calving into the ocean it has caused the global sea level to rise around 130 m since (Lambeck et al. 2014). North Jutland, including the Hesselø South area, was heavily affected by the isostatic depression during the last glacial period. The ice had pressed the land down into the asthenosphere creating a lower-lying area compared to before. When the ice sheets retreated 20,000 years ago, the global sea level gradually rose but because of the isostatic depression the regional water levels became relatively high even though the eustatic sea level was still at a low. As a result, fine sediments like clay and silt were deposited (Jensen et al. 2002). However, later the isostatic rebound together with the still rising sea level caused the regional sea level in Kattegat to be low. Bendixen et al. (2017a) conducted a study in the Hesselø area. In the period with low sea levels around 10.3-9.2 cal. ka BP they suggested an estuary environment where parts of the area were dry land or coastal wetlands. This was indicated by incursions of peat found in the area. Moreover, they found that the regression led to erosion due to coast activity and the formation of channels on land. Simultaneously, with the existence of the estuary, the Ancylus lake drained into the Kattegat through the Dana River (paleo-Great Belt channel) (see Figure 8). The Ancylus Lake was formed during the early Holocene as a result of the retreating ice sheets from the last glaciation. When the ice sheets melted large quantities of freshwater were released filling the

Baltic Basin (Björck 1995). Initially, the basin was isolated from the ocean creating a large freshwater lake known as Ancylus Lake, but it would later drain into the Kattegat. As the relative sea level continued to rise during the Holocene the Hesselø area was gradually flooded, meaning that the coast and subsequent systems moved further and further inwards (Jensen et al. 2002; Bendixen et al. 2017b). This led to the deposition of mud and gyttja in the deeper parts of the Kattegat.

3.3 Borehole data

Gardline has provided data from Hesselø that include descriptions of eight boreholes (BH) and 32 CPTs. From Kattegat II there is descriptions and plots from six boreholes and c. 20 CPTs. Only material from the boreholes have been available for the analysis and dating.

Borehole data from Hesselø South with interpreted soil type is available in preliminary reports from Gardline and Energinet. The boreholes vary in length from around 8m to 60m. Generally, the borehole samples are characterized by various layers of sand and silty to sandy clay. In a few borehole samples loose sand can be found in the top of the core which could correlate to the marine sands deposited in the Holocene. In other cores calcareous, silty clay is found in the top of the core. Clay deposits are often deposited in a deeper sea environment or in lagunes where energies in the water have been low enough for the accumulation of smaller grains. Some of the deeper layers of clay are characterized by being slightly gravelly. The gravel can be subangular to subrounded and it is of mixed lithology and grain size which may indicate glacial till. These layers can therefore be of glacial age.

By determining the lithology of the borehole samples and correlating these to the geophysical data the geological development of the area can be presented. The geological model can reveal periods of terrestrial environments and these are interesting in an archeological perspective. In a few cores clay with lenses of organic material is found. If the organic material comprises peat and is found in the right seismic horizon it may indicate a terrestrial environment where potential hunter-gatherer populations lived. However, a detailed review of the available core logs/plots from Hesselø has not yielded proof of any such layers (such as peat) representing former land surfaces.

4 Modelling sea levels

4.1 Collection of data

It is vital to understand the development of the landscape in a given region in order to be able to identify the parts of a project area that have the greatest archaeological potential. It is by no means a simple task to reconstruct the old coastlines in the Hesselø South area. One of the most important

reasons is that the extent of glacial isostatic rebound in the area is not yet clear. Because of differences in the rate at which land has rebounded from when it was pressed down by the glaciers it is simply impossible to reconstruct archaic coastlines across larger areas based on the modern bathymetric data. Additionally, from the Hesselø South area there are so few dated samples from cores and logs that the relative sea level rise is difficult to determine. It will therefore be vital to develop a shoreline displacement curve based on data from the area.

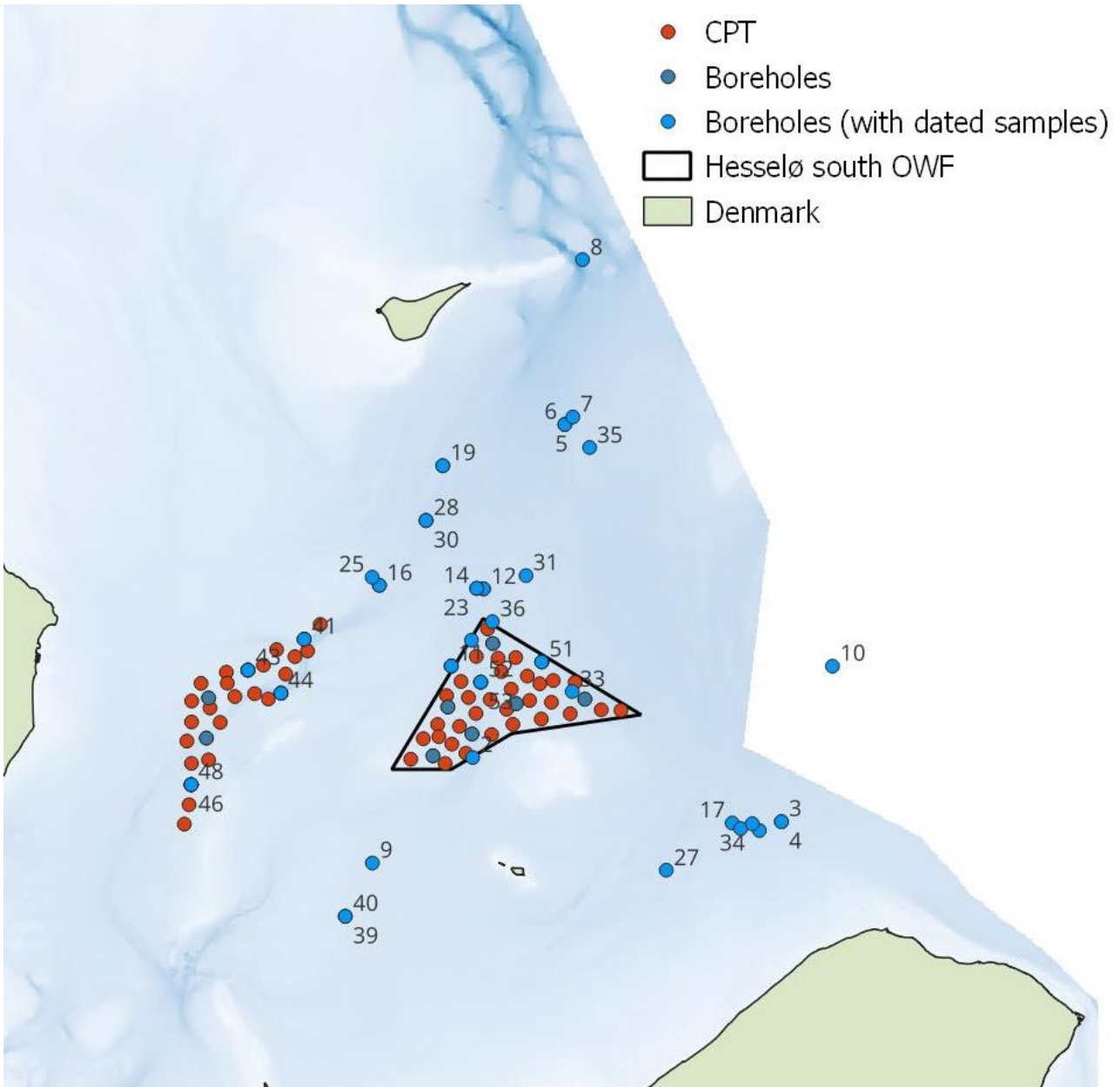


Figure 5. Borehole positions shown in blue (Numbers refer to ID number in Appendix 8.6. and sea-level curve in Figure. 6 and show dated samples. Cone penetration test (CPT) positions are shown in red.

To determine relative prehistoric sea levels it is crucial to have access to well-dated material. We have compiled an overview of dated samples from the Hesselø South area which are considered representative of the project area (see Appendix 8.6 and Figure 6). These include samples which were either directly above or below the sea surface during the Late Palaeolithic and Mesolithic and they can thus be used to bracket sea levels and coastlines at various points in the past. At some depth and age intervals there are few points that can be used to determine sea levels. To rectify this an agreement was reached between Energinet and MAV to date 11 samples from the Hesselø South area to enable poorly covered intervals to be addressed with much greater precision. 14 new boreholes have been made by Gardline within the Hesselø South OWF and Kattegat II area (see Figure 5). All core logs have been reviewed to identify samples from various depths for dating that are needed to produce a new shoreline displacement curve. MAV requested sediment samples from either marine or terrestrial layers based on the core logs. It turned out that the samples from Hesselø South only represent marine samples whereas a potential terrestrial sample (describes as peat) exist from Kattegat II. All samples were sent to Moesgaard Museum where they were sieved with the goal of recovering material best suited for dating. From the marine samples primarily marine molluscs were chosen for dating. Before being expedited for dating all shells were photographed to subsequently determine whether they come from marine, brackish, or freshwater environments. It was ascertained that the dated specimens was likely deposited below sea level at the time of deposition. It is often difficult to exclude if shells have been redeposited from where the animals originally lived/died and that pertains to the shells used in this study as well. Fragmented shells may indicate that layers are reworked/redeposited. On April 26th 2024, MAV delivered eight samples to the Aarhus AMS centre from Kattegat II and three samples Hesselø South. Moesgaard Museum received the results of these on the 20th of June 2024 (see Table 1 below).

Table 1 Radiocarbon dated samples from Kattegat II and Hesselø South. Contextual information about the individual samples can be found in Appendix 8.6.

AAR	Sample ID	Name	Material	Yield (%)	¹⁴ C Age ¹⁴ C yr. BP	Calibration Program	Calibration Options	Calibrated Age 95.4% (2σ)
38163	46762	HS_S_11_BH PO2 B1	shell	65,7	9101	4 2 OxCal v4.4.2 Bronk Ramsey (2020) ; r:5	Marine20 DeltaR: 52.0 ±25,0	7821BC (95.4%) 7460BC

MAV2023-050 Hesselø South

3816 4	46763	HS_S_11_BH PO1A	wood	52,9	8861	5 0	OxCal v4.4.2 Bronk Ramse y (2020) ; r:5	IntCal20	8228BC (95.4%) 7791BC
3816 5	46764	HS_S_06_BH PO2 T1 B3	shell	71,5	9057	4 8	OxCal v4.4.2 Bronk Ramse y (2020) ; r:5	Marine20 DeltaR: 52.0 ±25,0	7764BC (95.4%) 7386BC
3816 6	46765	KG_25_BH PO2 B2 x5	shell	78,3	4545	4 2	OxCal v4.4.2 Bronk Ramse y (2020) ; r:5	Marine20 DeltaR: 52.0 ±25,0	2757BC (95.4%) 2327BC
3816 7	46766	KG_25_BH PO2 B2 x6	wood	42,6	9148	5 3	OxCal v4.4.2 Bronk Ramse y (2020) ; r:5	IntCal20	8542BC (6.5%) 8511BC 8486BC (88.9%) 8275BC
3816 8	46767	KG_07_BH PO1 B2 x7	shell	57,1	2129	3 0	OxCal v4.4.2 Bronk Ramse y (2020) ; r:5	Marine20 DeltaR: 52.0 ±25,0	320AD (95.4%) 635AD
3816 9	46768	KG_07_BH PO1 B1 x9	shell	71,1	4207	3 4	OxCal v4.4.2 Bronk Ramse y (2020) ; r:5	Marine20 DeltaR: 52.0 ±25,0	2278BC (95.4%) 1897BC
3817 0	46769	KG_12_BH PO3 B2 x4	shell	77,3	7538	4 4	OxCal v4.4.2 Bronk Ramse y (2020) ; r:5	Marine20 DeltaR: 52.0 ±25,0	5976BC (95.4%) 5656BC
3817 1	46770	KG_25_BH PO1 B2 x11	nutshell	59,9	8871	4 5	OxCal v4.4.2 Bronk Ramse y	IntCal20	8231BC (82.6%) 7931BC 7923BC (12.8%) 7820BC

							(2020) ; r:5		
3817 2	46771	KG_25_BH PO1 B2 x10	shell	79,7	4815	3 2	OxCal v4.4.2 Bronk Ramse y (2020) ; r:5	Marine20 DeltaR: 52.0 ±25,0	3066BC (95.4%) 2681BC
3817 3	46772	KG_02_BH PO3 B2 X8	shell	76,7	4230	3 1	OxCal v4.4.2 Bronk Ramse y (2020) ; r:5	Marine20 DeltaR: 52.0 ±25,0	2305BC (95.4%) 1925BC

4.2 Modelling sea levels – creating a shoreline displacement curve

A shoreline displacement curve shows relative sea levels at various points in time in relation to the current level. The curve that was made for this project is based on both existing dated samples (for example, those produced in connection with the Thor offshore windmill project) and others collected specifically for the Energy Island (EI) and OWF projects. For samples to be included in the analysis they must meet the following criteria:

- 1) they provide information about prehistoric sea levels
- 2) they have been recovered in a secure context (*in-situ*)
- 3) they have available vertical placement information
- 4) they are absolutely dated (e.g. with radiocarbon dating).

Table 1 shows the results of the radiocarbon dates from the planned area. Additional contextual information about the dated samples can be found in Appendix 8.6. while Figure 5. shows the spatial distribution of radiocarbon dated sea-level index points used to develop a new sea-level curve. ¹⁴C-ages are reported in conventional radiocarbon years BP (before present = 1950) in accordance with international convention (M. Stuiver & H.A. Polach: Discussion of reporting ¹⁴C data. Radiocarbon 19 (3) (1977) p. 355). All calculated ¹⁴C ages have thus been corrected for fractionation so as to refer the result to be equivalent with the standard δ ¹³C value of -25‰ (wood). δ ¹³C values have been

measured by AMS only and are not reported since the values obtained here are not as precise and therefore only indicative regarding association with the terrestrial, marine, or freshwater food chains.

The sea level curve is created by entering the uncalibrated ^{14}C -dates and vertical placement information (masl) into an Excel spreadsheet after which it is imported into the online calibration software OxCal. The dates were modelled in OxCal after age and vertical location using the depth model function. Samples are calibrated and shown in the shoreline displacement curve with a 95.4% confidence interval. Previous dates that were done at the radiocarbon lab in Copenhagen on marine samples have a built-in correction for the marine reservoir effect, so no additional correction was done for this study. The marine samples that were dated at the AMS laboratory in Aarhus and other laboratories are corrected with a reservoir effect of 400 years. All the dates are calibrated after the new IntCal 20 curve (Reimer et al. 2020) and they are plotted in the curve by comparing the vertical location versus age.

The shoreline displacement curve in Figure 6 shows marine samples in blue (for example, marine shells), terrestrial samples in green, and samples coming from sand layers which may come from the coast or a lakeshore in grey. All the fixed points on the curve were assigned a number (R_Data) that can be referenced in Appendix 8.6. (column “id”) so it is possible to see additional information about the individual samples that are dated. The curve clearly shows that sea levels rose dramatically during the earliest part of the Holocene period. This indicates that all land surfaces were transgressed during the Maglemose culture (9,000-6,400 BC) at the latest and that any human presence during the Kongemose (6,400-5,400 BC) and Ertebølle (5,400-4,000 BC) cultures can be excluded.

Another sea level curve that represents the area was presented by Jensen and Bennike (2020) (Figure 7). It suggests that the relative sea-level fell until c. 10,000 cal BC when it reached a level approx. 30-35 m below that of today. (This corresponds to the lowest recorded terrestrial sea level index point (SLIP) used in Figure 6). If the sea-level curve is representative there should be little to no archaeological Stone Age potential in the areas of the OWF that lies deeper than 30-40 m. Both sea-level curves also suggest a sea-level rise in the area from at least 11,000 cal BC. However, a notable lack of terrestrial SLIPS within the area makes it very difficult to determine the prehistoric sea-level with sufficient details.

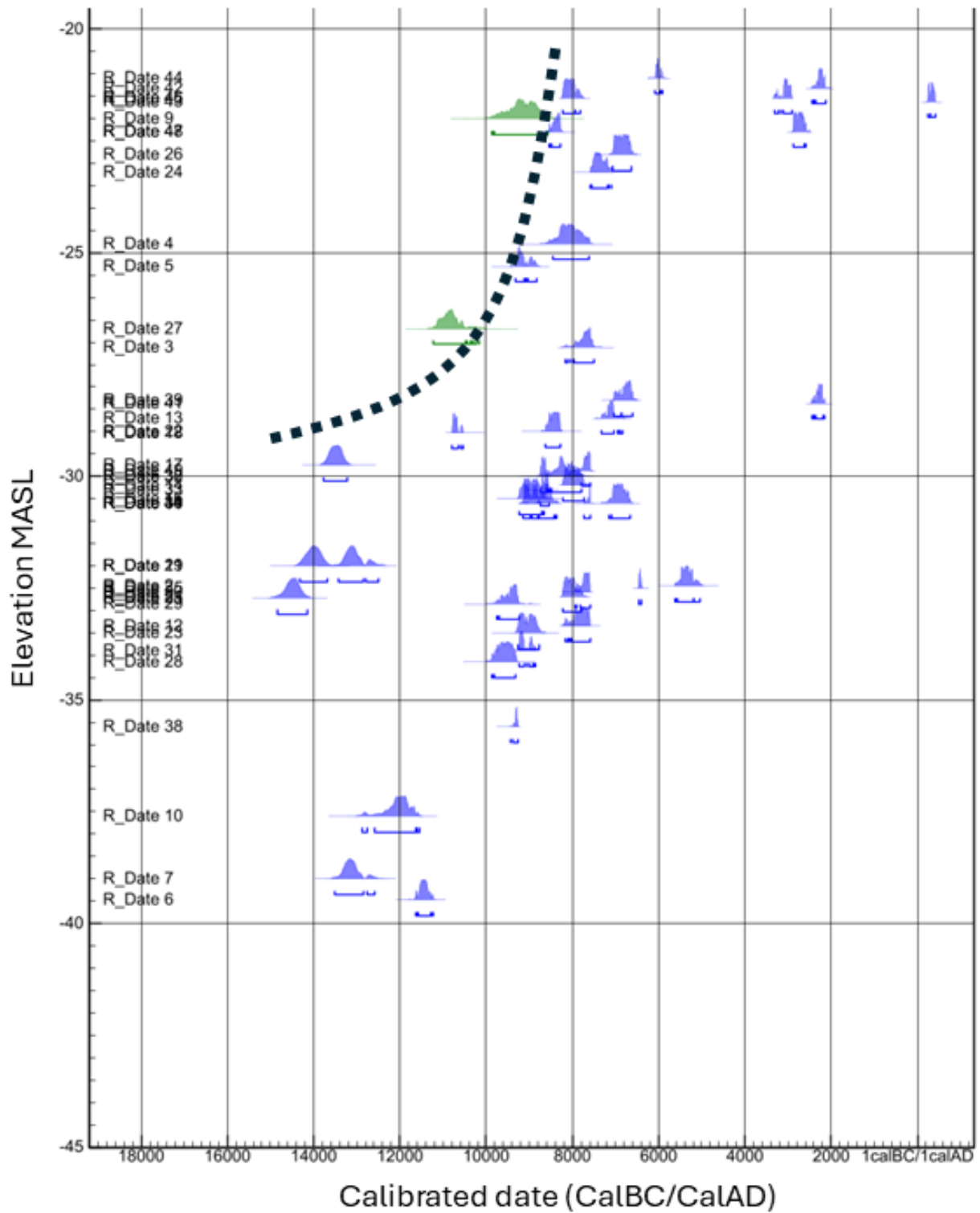


Figure 6. Sea-level curve where the dashed line gives the hypothesized sea level in the planned OWF area during the Holocene. Marine samples are shown in blue whereas terrestrial samples are shown in green.

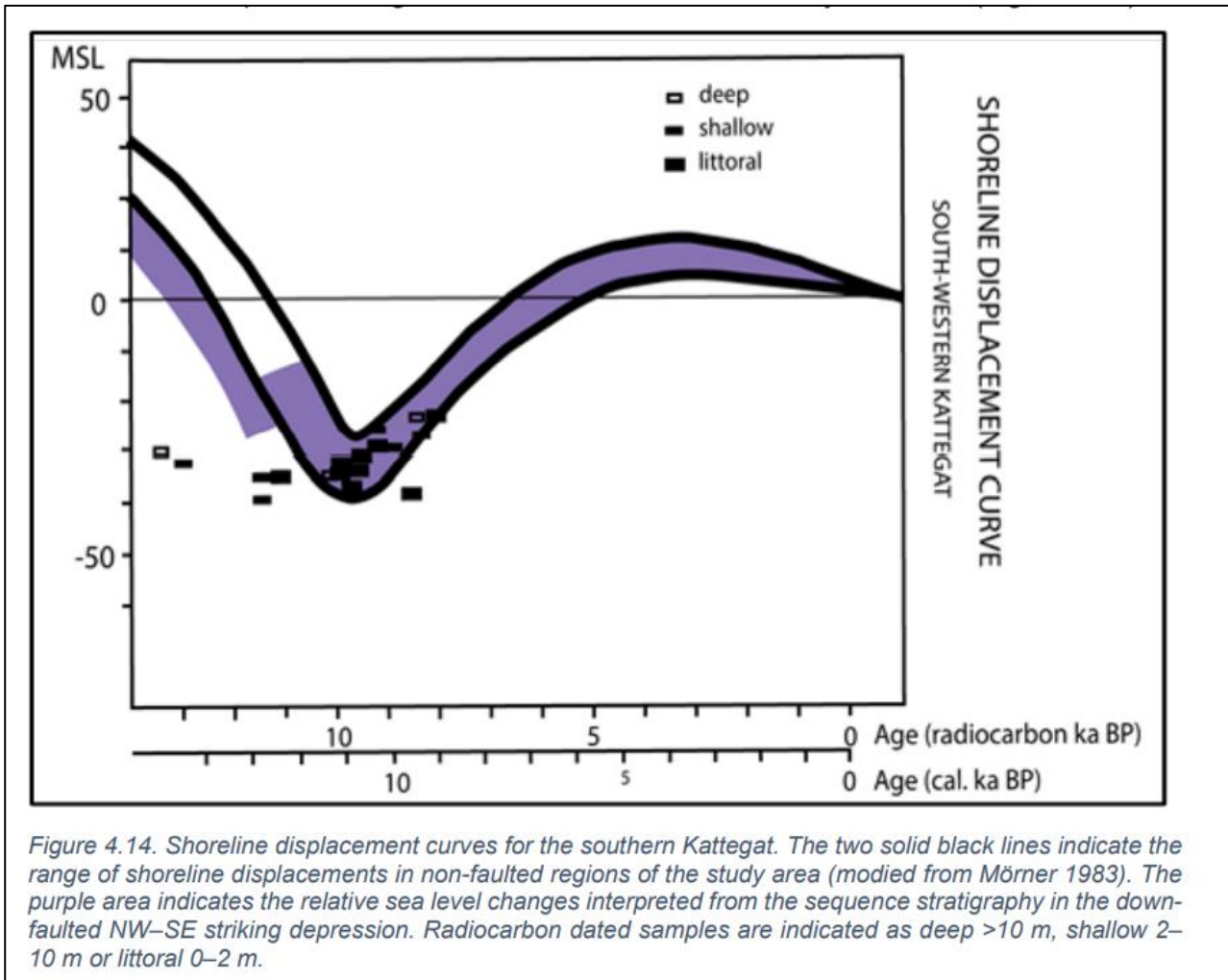


Figure 7. Sea-level curve from Jensen and Bennike (2020).

Figure 6 shows the new sea level curve where the dashed line gives the hypothesized sea level in the planned OWF area in the Holocene. Furthermore, Table 2 summarizes the sea levels at different times as they appear on the curve. It can be seen from the curve that there is a relatively good correlation between the marine and terrestrial samples with the latter typically situated above the marine. It is difficult, however, to determine sea levels more precisely than $\pm 5\text{m}$ as the samples' vertical reference does not typically correlate precisely with that in the past. On top of that is the uncertainty associated with dating shells and peat combined with the yet long intervals where there are few dates available for determining sea levels. Another issue affecting placement of the curve is the isostatic rebound which has changed the vertical position of the samples used in the shoreline displacement reconstructions. Generally, lands to the north-east of the OWF area have been lifted more than those to the south-west. Thus, it is problematic to include points from a wide geographic area. The degree

of difference in rebound within the area is not known precisely, and it is therefore not corrected for in this curve.

Table 2 Sea-levels estimated from the sea-level curve.

Time cal BC	Sea-level
7500	-15,0 m
8000	-18,0 m
8500	-21,0 m
9000	-24,0 m
9500	-25,5 m
10000	-26,5 m
10500	-27,5 m
11000	-28,0 m
?????	-30,0 m

4.3 Sub-bottom seismology and landscape correction

A report provided by GEOxyz presented 4 seismic surfaces/horizons. These have been used to identify the seismic units. In the geological desk study made by *De Nationale Geologiske Undersøgelser for Danmark og Grønland* (GEUS) several seismic and lithological units are presented. These constitute the geological model in the area which has been used to build upon in the geophysical report. Horizons represent the boundaries between different layers of sediment in the subsurface and the different layers of sediment each represent a unit. Each unit represent a layer of sediment deposited in a specific depositional environment. Borehole data can determine the type of the sediment and help determine past environments. By comparing a sequence of units, the geological development can be recreated. The units and horizons are important for understanding the geology in coastal areas as different sediments can affect erosion and sedimentation and thereby determine where the coast was located. The lowest elevation in any of these horizon grids (tiff's) is therefore used to model the old coastline position as they give a better picture of the prehistoric landscape than the modern seabed. Therefore, this data can help determine where paleo-coastlines were located.

In the geophysical survey report provided by GEOxyz, 4 different main units were presented. The geophysical study has been interpreted with reference to sediments and unit names used in the geological desk study by GEUS. As highlighted in the geological report (SCREENING OF SEABED GEOLOGICAL CONDITIONS FOR THE OFFSHORE WIND FARM AREA HESSELØ SOUTH AND THE ADJACENT CABLE CORRIDOR AREA. DESK STUDY FOR ENERGINET), the ages of the horizons are associated with uncertainties and relative to each other as it is not possible to know the precise age from the seismic data. Unit IV is the oldest unit presented in the geophysical report and it comprise the bedrock. The top of the bedrock is found 40-50 m below seabed. The unit consists of carbonates of Cretaceous age and clastics of Jurassic age. Numerous faults are found in the seismic data of this unit. Unit III is found on top of unit IV and it is expected to have been deposited during the LGM. It consists of variable glacial till and the upper part of the unit has been subjected to ice contact. Unit II is expected to have been deposited in the Late Weichselian to early Holocene. The unit consists of laminations of clay and sand. The uppermost unit, Unit I, is of Holocene age and it deposited in a marine environment. Unit I comprise silty, sandy clay and thin sandy seabed sediments.

The unit which is relevant for archaeology is the terrestrial unit as it plausibly contains preserved archaeological material. Because the depositional environment is expected to have been periglacial to glaciomarine the unit with potential for archaeology is therefore Unit II (or Unit B as it is called in the desk study GEUS). The horizon that marks the bottom of this unit is H20. As seen on Figure 10, the horizon is closest to the seabed in the south-western and south-eastern corner of the project site. Unit II is very complex due to the varying environmental conditions during the Late Weichselian and early Holocene. It consists of laminated clays and silts, sandy beach-type deposits, and indications of late ice contact. To the southwest, the glaciomarine sediments are thinning over thick subcropping tills. These form a delta-like complex of deposits sourced from the south. This is supported by the depositional environment of Unit B being interpreted by Jensen et al. (2023) to be an estuary environment situated at the mouth of the Dana River System (see Figure 8). This river system drained the Ancylus River into the Kattegat as explained in chapter 9. This may, furthermore, indicate that parts of this horizon were once terrestrial. The lower deposits of Unit III show a stronger ice influence, while the later deposits of Unit II holds preserved bedded facies with limited ice contact. In the northern part of the study site Unit II is thinning over an east-west trending till ridge (Unit III), identified as the Sjællands Odde ice marginal ridge. North of this ridge, glaciomarine deposits form a knoll and could have been pushed against the till ridge by a later ice advance from the Baltic Ice

Stream. These northern deposits have a more chaotic internal structure compared to that south of the ridge.

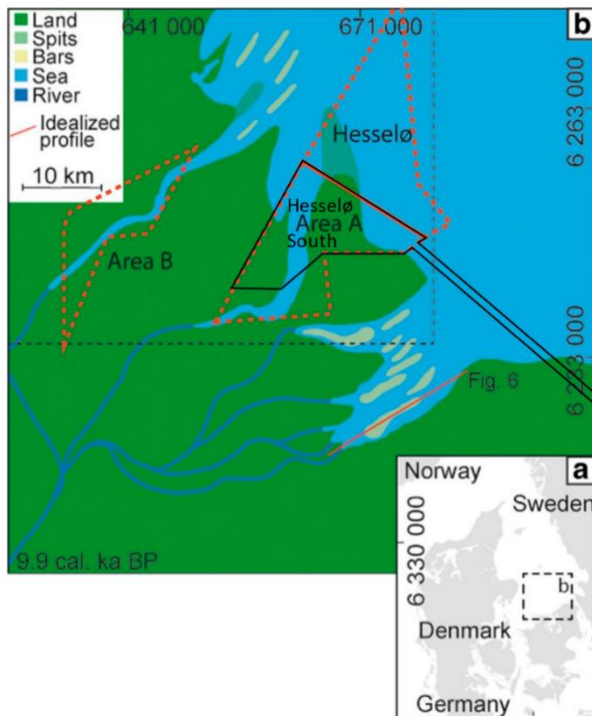


Figure 8. Depositional environment for Unit B including several estuaries, back-barrier basins, bars and spits. Hesselø South area and cable route are marked by a black line. Moreover, the previous Hesselø area and Area B is marked by a red dotted line.

The morphology of the H20 horizon fits somewhat well with the geological model presented by Bendixen et al. (2017a). The paper suggest that the Hesselø South area functioned as an estuary environment as the transgression progressed from the north. This is plausible as the south-western and south-eastern parts of the H20 horizon within the project site are located higher up than the rest of the horizon and would thereby be flooded later.

4.4 Coastline Models

When correcting for the changes (sediment transport, erosion/accumulation) that have occurred in the Hesselø South site since the Stone Age it is vital to use the most suitable horizon. For example, if there are traces of buried valleys/lakes in a horizon it is crucial to correct for them. Alternatively, there is a risk of giving these areas a misleading influence on the results (and lead possible marine archaeological investigations to the wrong locations). The geophysical report considers Unit II to have formed as a result of the area transgressing in the late glacial and Holocene period. The lowest elevation in this horizon grid (H20) is therefore used to model the old coastline position as it gives a

better picture of the prehistoric landscape than the modern seabed. Where two horizons lie above each other we have used the oldest marine horizon with the lowest elevations. The different coastlines shown below in Figure 11-15 are thus all drawn manually in QGIS to follow a certain depth in a horizon grid considered to be the most representative of the old land surface. We chose to make three maps with different sea levels (15m, 20m and 25m) corresponding to the time intervals around 7,500, 8,400, and 9,400 CalBC respectively. It is uncertain if the water level has been lower than 30 m below present-day sea level (and when) but a hypothetical model is presented to account for this scenario (Figure 15). The new coastline models are very different from the one in Figure 8 as they show less land. A possible explanation is that the depicted coast in Figure 8 is based on the modern bathymetry (Figure 9), whereas the new coastline models are drawn according to H20 (= lower elevations). The current water depth is between -17 m and -35 which means that a much larger part of the area had been depicted as land if the modern bathymetry had been selected as analogy for the old land surface.

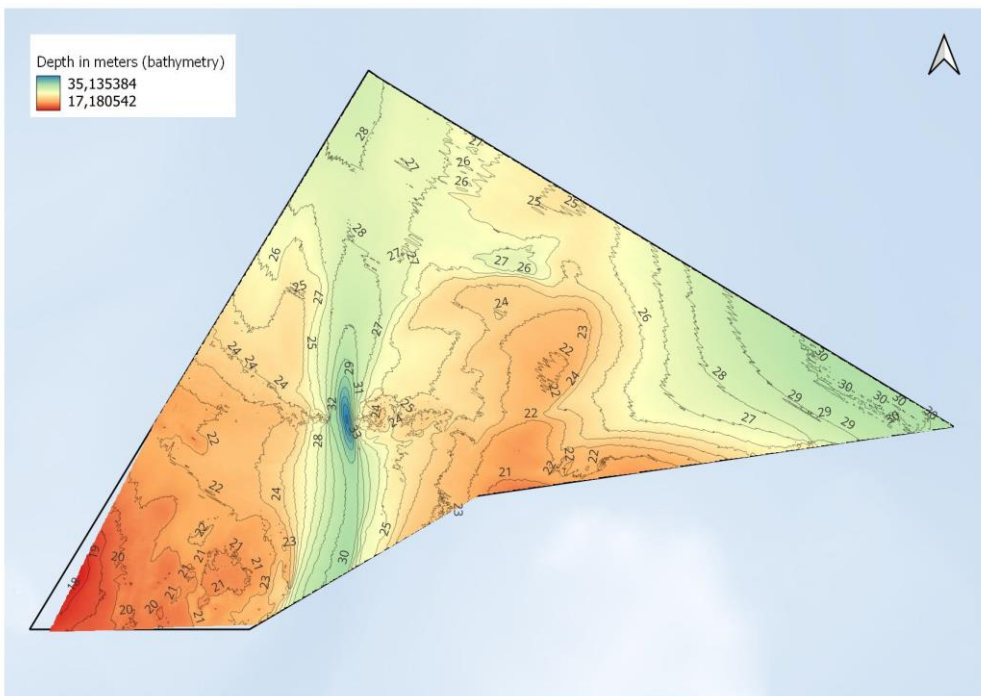


Figure 9. Modern bathymetry in the Hesselø South OWF area.

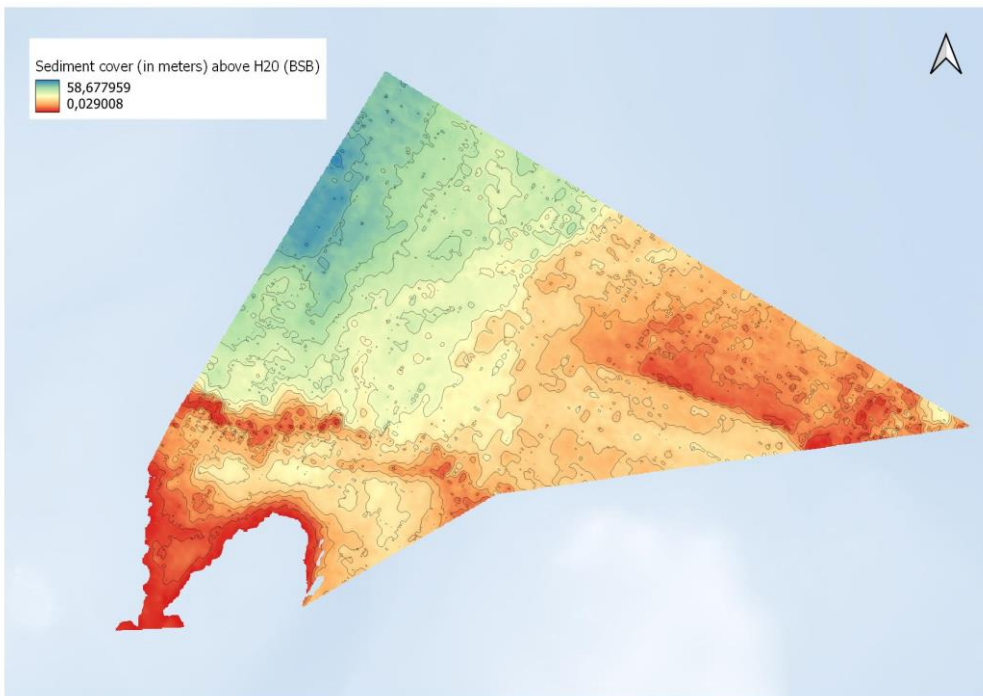


Figure 10. Distance from seabed to H20 in meters. The lowest/deepest areas recognized on H20 are important because they can be thought to represent lake basins that are filled with sediment. The material that is deposited over the archaic lake basins, peat layers, etc. both preserves them and makes them difficult to research. Higher areas on slopes are more exposed and subject to erosion but are also better suited to diver reconnaissance precisely because settlement traces are not buried under a thick layer of sediment. Identification of the areas with the greatest Holocene layer formation shows both 1) where archaeological materials can have avoided erosion, 2) where it would be difficult to access layers using divers, and 3) where layers are too deep to be affected by construction work. Therefore, archaeological surveys should be planned in the areas best suited for settlement where past sedimentation allows such investigations without extreme difficulty in accessing the layers.

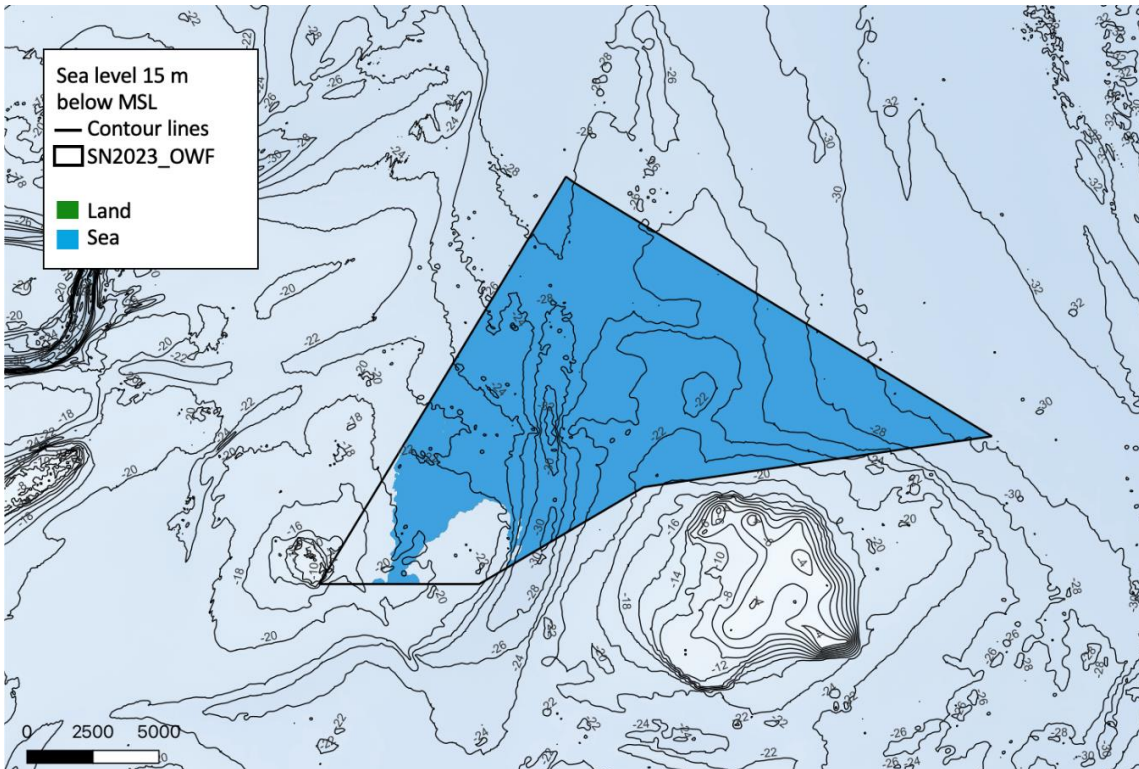


Figure 11. Coastline position at -15 m below msl corresponding to the time around 7500 cal BC. Drawn according to the lowest postglacial horizon H20. As it can be seen the area was completely transgressed at this time.

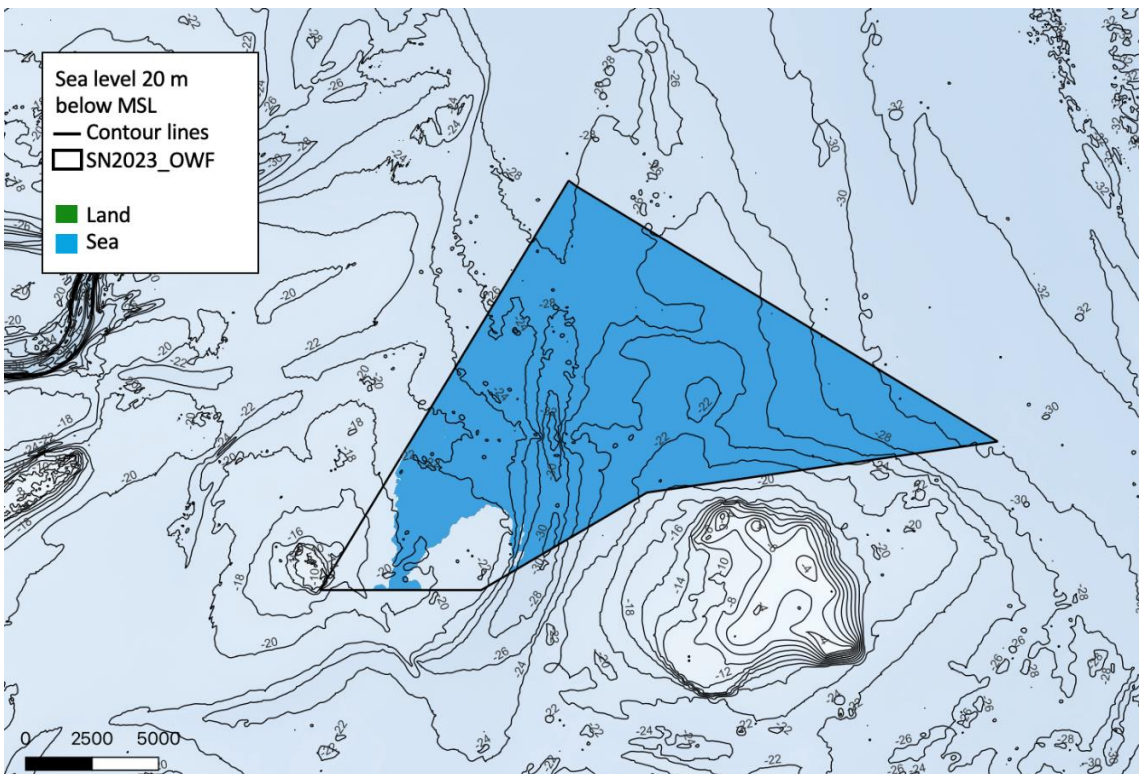


Figure 12. Coastline position at -20 m below msl corresponding to the time around 8400 cal BC. Drawn according to the lowest postglacial horizon H20. As it can be seen the area was completely transgressed at this time.

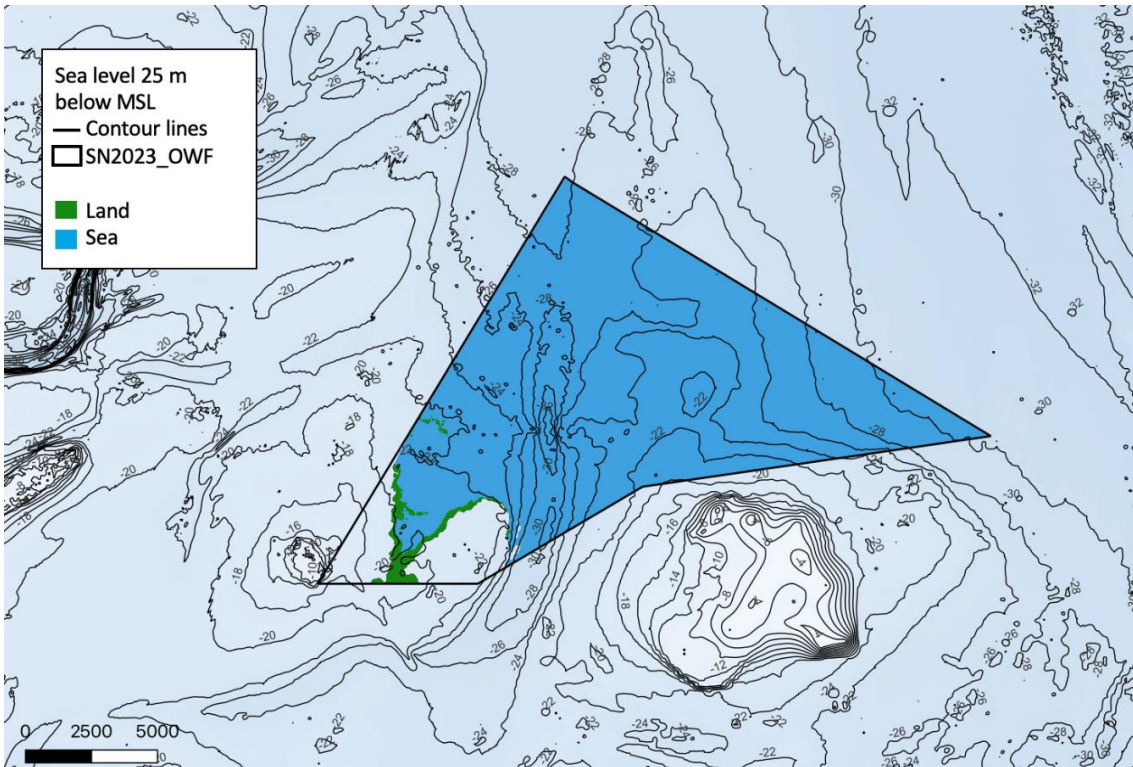


Figure 13. Coastline position at -25 m below msl corresponding to the time around 9400 cal BC. Drawn according to the lowest postglacial horizon H20. As can be seen from the model there might have been an exposed land surface in the southwestern corner.

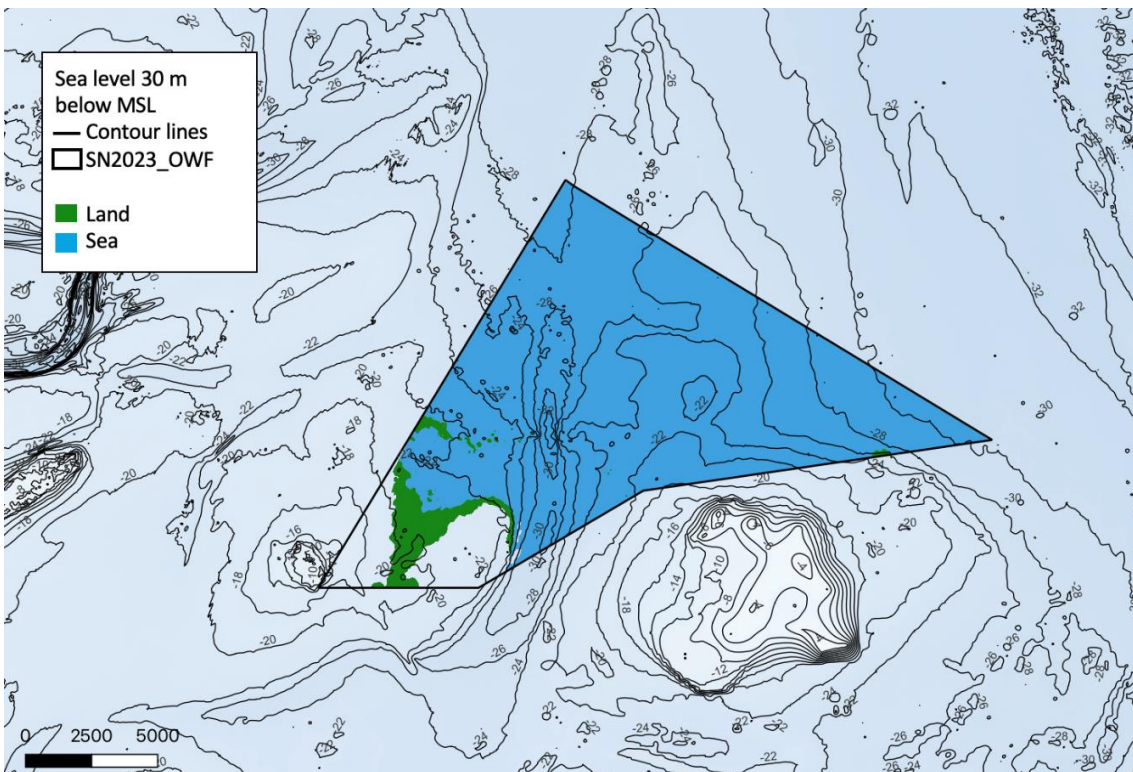


Figure 14. Coastline position at -30 m below msl. Drawn according to the lowest postglacial horizons H20. It is uncertain if the water level has been as low as modelled.

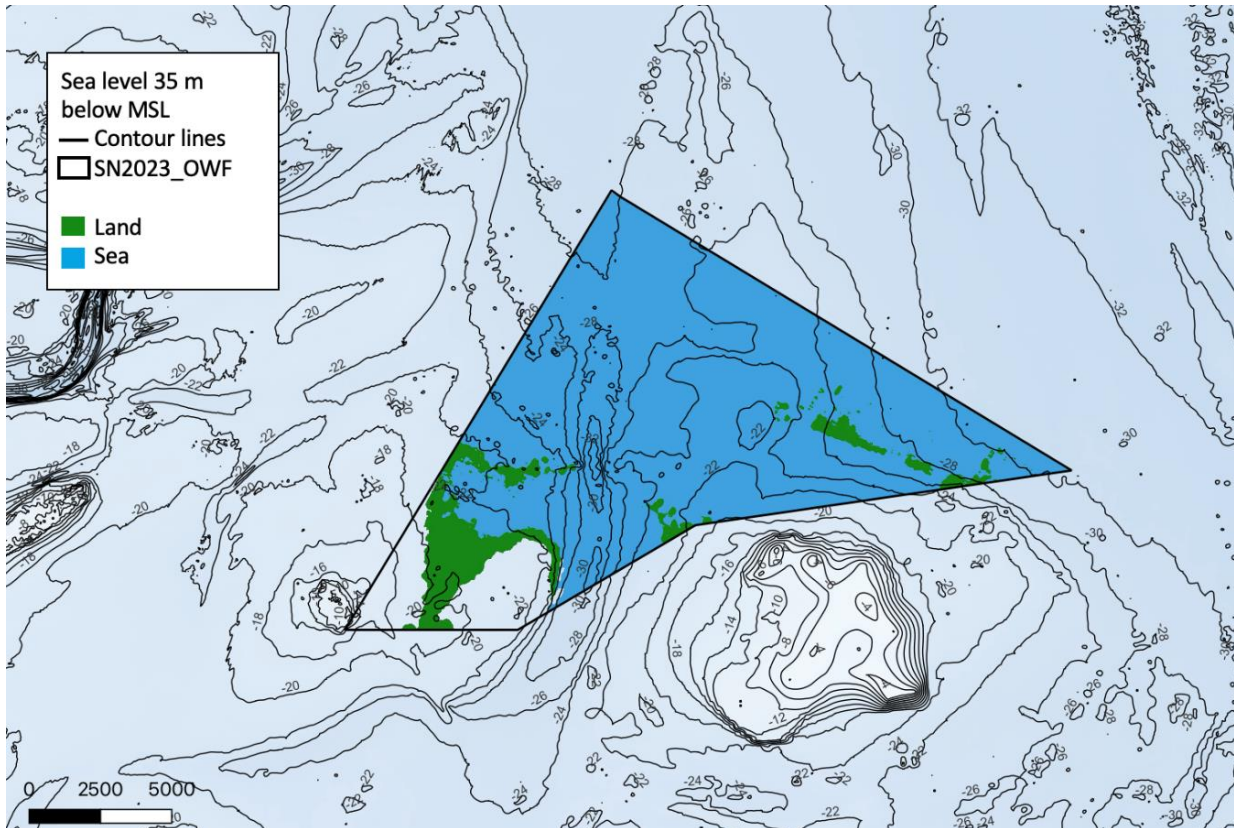


Figure 15. Coastline position at -35 m below msl. Drawn according to the lowest postglacial horizons (H20). It is uncertain if the water level has been as low as modelled.

It appears from the new coastline models that the area changed radically due to the transgression. It can be seen when the different parts of the areas were transgressed and made uninhabitable. The models show that with a sea level 20 m below today's mean sea level the area would have been completely flooded (if H20 is used as analogy to the prehistoric land surface). At a sea level 25 m below MSL a few areas to the south-west would have been land areas on H20. It is also likely that the area with no data in H20 was land. At a hypothetical sea level of c. 35 m below MSL various areas would have been land.

The coastline models can be compared to Figure 8, which was presented by Bendixen et al. (2017a). On Figure 8, the morphology of the horizon even shows a deeper area in the middle of the site striking north/south, which could indicate a channel system as suggested by Bendixen et al. (2017a) (Figure 8). This would further support the hypothesis that the depositional environment was an estuary. It can, however, be difficult to determine the channel solely from the topography of the horizon.

The Stone Age potential in the mapped land surfaces also depends on the distance from the modern seabed to layers with the Stone Age potential. (as the layers should be reachable with the available

methods). Figure 10 shows how much marine sediment that has been deposited since the areas were inundated. It appears that the sediment cover on top of H20 varies from 0 to 58m. Likewise, it has been listed in Appendix 8.6 how much sediment is accumulated on top of the dated samples in the boreholes. The isopach grids and boreholes does, therefore, show where it is difficult to reach layers with archaeological Stone Age potential and where it is unlikely that cables etc. will cause any damage to them.

4.5 Areas of archaeological interest

Normally, in a geoarchaeological analysis the reconstructed landscape would be used with topographic models (e.g., the fishing site model) to designate areas with a particularly high likelihood of human activity having taken place. However, the topographic model is deemed an unsuitable tool for finding settlements as the geological data from the Hesselø OWF area only provide very limited information about the most favourable topographical locations in the area, the reason being that potential settlements would have been so old (min 11,000 years ago) that it is unclear if the topographical models apply. Furthermore, we still know too little about the area's original topography and environment, it is unknown whether the landscape consisted of large, exposed beaches subjected to powerful surf (and with long stretches uninterrupted by bays or lagoons), or if it to a greater extent resembled the landscapes and environments found today in the inner Danish waters such as the Belts. Known traces of the early Mesolithic societies in southern Scandinavia have primarily been located along former lakes and river systems later changing into bogs. (That is particularly so in the bogs of northeast Zealand). There are equally good reasons to believe that people favored wetland areas in the Hesselø South area if such existed. However, none of the boreholes in the Hesselø South area have contained peat deposits. Peat represents preserved land surfaces and thereby indicates areas with excellent preservation conditions for organic material (wood, bone etc.). The boreholes have instead proven that clay and marine sediments are distributed across most of the area.

5 Cultural historical archaeology

5.1 Methods

Geophysical data provided by Energinet was used for the geoarchaeological analyses. The comprehensive specifications for the data collection, equipment, technical details, data processing, and interpretation methods can be found in the report "Geophysical Surveys For Danish Offshore Wind 2030 - Hesselø South" by GEOxyz and provided by Energinet.

Magnometer (MAG) anomalies were delivered in various formats (see B06 below) and SonarWiz files had embedded file paths that needed to be manually corrected where possible to have access to all features.

SSS-data was primarily used for analysis to identify potential cultural historical objects.

Anomalies were chosen based on whether their character indicated potentially man-made objects that were lost over 100 years ago and therefore protected by the Danish Museum Act. The SSS-data was analysed in SonarWiz from which the targets and information were exported and further manipulated in QGIS and MS Office.

SSS anomalies were first marked in SonarWiz on the first data delivery where anomalies were not preselected by GEOxyz. When the revised data package was delivered the selection made by the maritime archaeologist was compared to the selection by GEOxyz. The selection by GEOxyz was accepted as reliable, therefore the analysis was focused on anomalies which had already received a designation as other than “Boulder”. Nonetheless, the anomalies designated as “Boulder” by GEOxyz were taken into consideration when they correlated with MAG or multibeam echo sounder (MBES) anomalies or otherwise with points of interest.

MAG-anomalies with a peak-to-peak (P2P) value of 40 nT or greater were automatically selected for further inspection, although the anomaly list includes those associated with known modern shipwrecks of ARCHAEOLOGY CONFIDENCE 4 (see below). B06 MAG-anomalies were delivered without P2P-values and therefore, all 185 anomalies listed in the SonarWiz file are included in the MAG-anomaly list. MBES-anomalies were not inspected individually unless associated with an SSS and/or MAG-anomaly.

The SSS-anomalies, in addition to the classifications used by GeoXYZ in SonarWiz, were divided into four categories indicating their importance and likelihood as cultural historical objects.

CONFIDENCE 1 refers to anomalies which most likely represent archaeological objects. The anomaly needs to be inspected and/or a safety zone needs to be established around it so that the project does not conflict with the object. The size of the zone will depend on an evaluation of the specific object/site.

CONFIDENCE 2 refers to anomalies that are more uncertain. This category includes the most interesting anomalies for a maritime archaeological survey. The anomaly should be investigated and/or avoided.

CONFIDENCE 3 refers to anomalies whose character cannot be determined, that is objects which are just as likely to be modern debris as archaeological artefacts. There is a probability that some of these objects are geological features/boulders. Linear features, such as ropes, which SSS-contacts associated with buried MAG-anomalies often fall into this category. The anomaly should be investigated and/or avoided.

CONFIDENCE 4 refers to anomalies which most likely represent modern debris. This may be debris associated with fishing, such as parts of trawl equipment. Linear objects with a large MAG-anomaly suspected of being wires or soft ropes with metal threads are included in this category. Anchor chains fall into the CONFIDENCE 3 category. Trawl marks were also taken as indication of the age of anomalies. Where trawl marks, seen as modern, ran underneath an anomaly, the anomaly was interpreted as modern and put into the CONFIDENCE 4 category. The anomaly does not require investigation or an archaeological exclusion zone (AEZ = areas where anchoring and operations are prohibited during construction and no infra-structure may be placed within the zone) but is still, if applicable, protected by paragraph § 29 h. of the Danish Museum Act. Geological anomalies were not marked separately.

Objects in the categories CONFIDENCE 1 and 2 are of archaeological interest and MAV recommend that these are investigated if they are to be disturbed by the construction work (or other work phases). Investigation of CONFIDENCE 3 anomalies can be omitted if necessary due to other constraints. This should, however, be done in agreement with MAV. CONFIDENCE 4 anomalies are included in the table because, despite being of recent origin some of them may reach an age of 100 years in the future which will put them under protection by the Museum Act.

It is up to SLKS to decide which of the above-mentioned anomalies that are to be inspected and possibly protected as part of an archaeological pre-survey. It is also the role of SLKS to define exclusion zones around wrecks and anomalies etc.

5.2 Results

There are 310 SSS-anomalies detected in the project area. Out of these, 13 are designated CONF 1, 34 are designated CONF 2, 196 are designated CONF 3 and 67 anomalies are designated CONF 4 (most likely modern (MMOs)).



Figure 16. The wreck of UMINI on the SSS-mosaic

5.2.1 SSS-anomalies

Based on the above, MAV proposes that SLKS sets conditions for the project to work around the anomalies in categories CONF 1-3.

The museum recommends as optimal mitigation to investigate the anomalies to further evaluate how the object should be interpreted and determine more precisely an appropriate AEZ. Alternatively, MAV recommends that the following exclusion zones be established around the anomalies:

- CONF 1: 200 meters in diameter (measured from centre where applicable, measured from maximum outer dimensions where applicable)
- CONF 2: 100 meters in diameter (measured from centre where applicable, measured from maximum outer dimensions where applicable)
- CONF 3: 50 meters in diameter (measured from centre where applicable, measured from maximum outer dimensions where applicable)

The size of the AEZ is set in relation to the anomaly's category and interpretation. An inspection of the anomaly could refine the designated zone, reducing it if it is a smaller, unified object or removing it altogether if it is not of cultural historical interest.

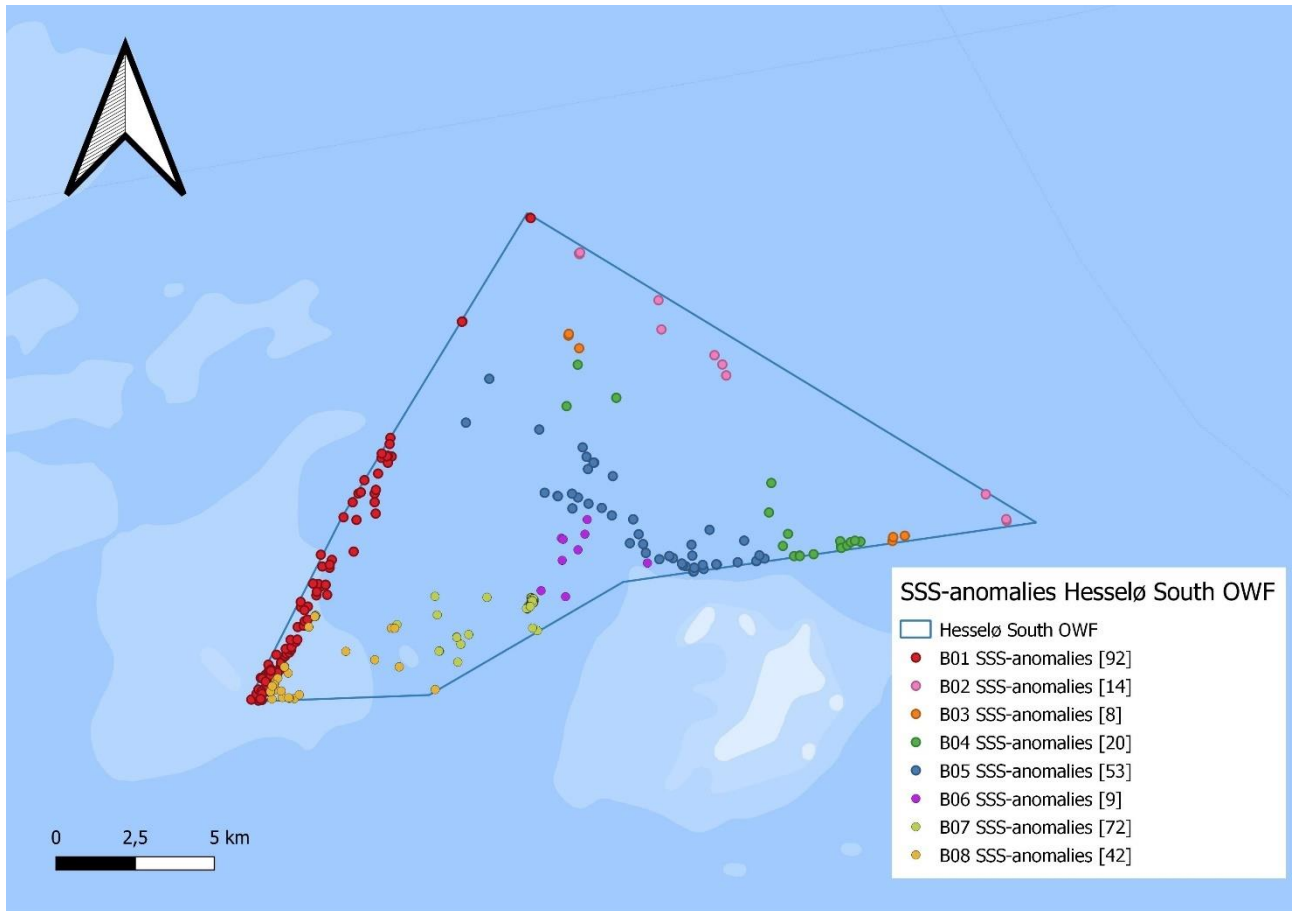


Figure 16. Map over the SSS-anomalies.

Among the anomalies is one potential anchor (HS_B04_SSS_GO6_0707) and 3 anomalies interpreted as shipwrecks (HS_B02_SSS_GO6_0523, HS_B03_SSS_GO6_0106, HS_B05_SSS_GO6_0291). Furthermore, anomalies are selected as the best possible matches to locations in the *Fund og Fortidsminder* (FFM) archive. These locations should be inspected and are otherwise classed as CONF 2.

5.2.2 MAG-anomalies

All magnetic anomalies with a peak-to-peak value of 40nT or more were selected for inspection with a few additional anomalies selected based on individual assessment of associated SSS- or MBES-features. 283 anomalies are listed including 185 anomalies without P2P-values from B06. The selected MAG-anomalies are listed in Appendix 8.4.

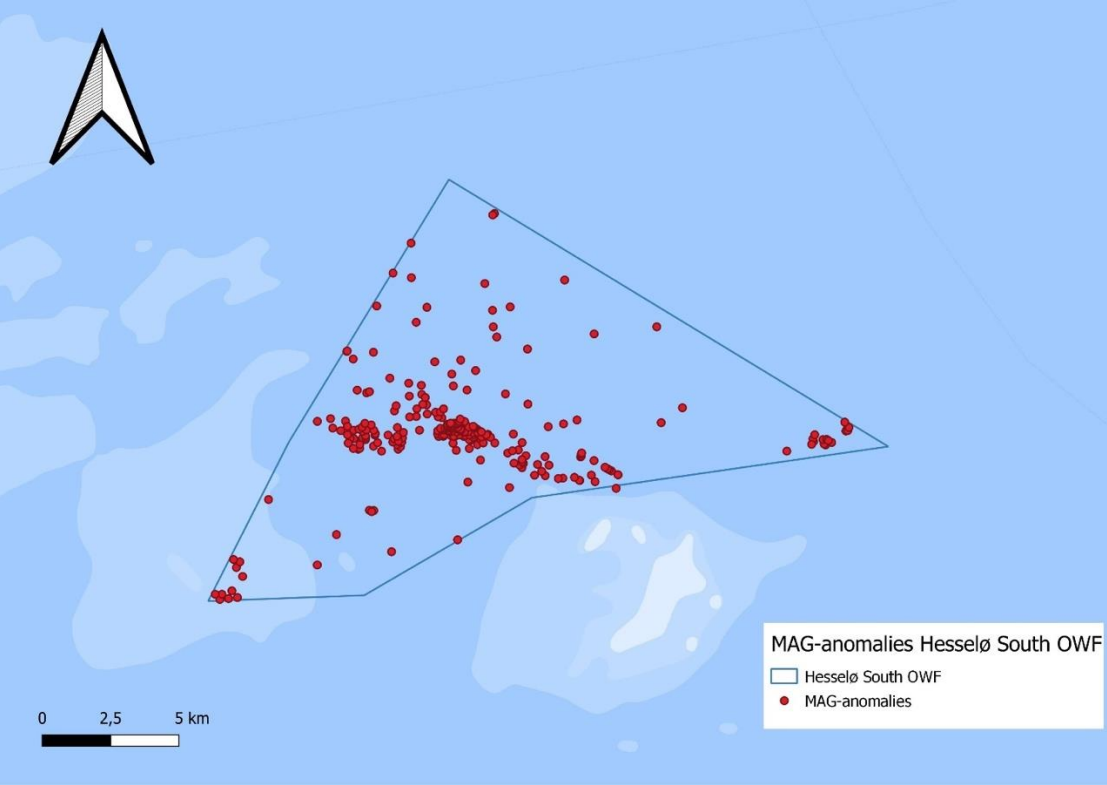


Figure 17. Map over the MAG-anomalies.



Figure 18. The wreck of BORINGIA with the MAG-tracks overlaid on top of the SSS-mosaic.

6 Conclusions

Possible Stone Age sites in the project area date to the Late Palaeolithic or Early Mesolithic as it was inundated by rising sea levels no later than 9,400 cal BC. Even before 9,400 cal BC the area might only have been habitable for a couple of thousands of years. As there are generally few sites known from these periods in the rest of Denmark it is considered unlikely that a sampling program at Hesselø South will succeed in finding significant additional archaeological material (not least considering the methods that would have to be employed to recover such material). The geoarchaeological analysis imply that construction work do not pose a threat to prehistoric settlements. We cannot exclude the possibility that there have been humans within a small area (and depth interval), but we do not believe there is sufficient justification for an attempt to detect them. Consequently, we will not recommend SLKS that any archaeological pre-investigations are conducted with the intention of identifying potential Stone Age sites in the OWF area.

MAV recommends the ROV and/or diver investigation of CONF 1 (n=13) and CONF 2 (n=34) anomalies as well as the mitigation of CONF 3 (n=196) anomalies by AEZ. The investigation of the anomalies can be combined with a potential unexploded ordnance (UXO) investigation and removal campaign. MAV recommends a maritime archaeological supervision for potential UXO investigations, as these will likely concern some of the anomalies listed in this report.

Literature:

Andersen, S. H. (2013) Tybrind Vig. Submerged Mesolithic settlements in Denmark.

Astrup, P. M. 2018. Sea-level change in Mesolithic southern Scandinavia. Long- and short-term effects on society and the environment. Jutland Archaeological Society Publications Vol 106, 2018.

Bendixen, C., Boldreel, L. O., Jensen, J. B., Bennike, O., Hübscher, C., & Clausen, O. R. (2017a). Early Holocene estuary development of the Hesselø Bay area, southern Kattegat, Denmark and its implication for Ancylus Lake drainage. *Geo-Marine Letters*, 37(6), 579–591. <https://doi.org/10.1007/s00367-017-0513-7>

Bendixen, C., Jensen, J. B., Boldreel, L. O., Clausen, O. R., Bennike, O., Seidenkrantz, M., Nyberg, J., & Hübscher, C. (2017b). The Holocene Great Belt connection to the southern Kattegat,

- Scandinavia: Ancylus Lake drainage and Early Littorina Sea transgression. *Boreas*, 46(1), 53–68. <https://doi.org/10.1111/bor.12154>
- Björck, S. (1995). A review of the history of the Baltic Sea, 13.0-8.0 ka BP. *Quaternary International*, 27, 19–40. [https://doi.org/10.1016/1040-6182\(94\)00057-C](https://doi.org/10.1016/1040-6182(94)00057-C)
- Erlström, M., Kornfält, K.-A. & Sivhed, U., 2001: Berggrundskartan 2D Tomelilla NO/2E Simrishamn NV. Sveriges geologiska undersökning Af 213.
- Fairbanks, R.G. 1989, A 17,000-year glacio-eustatic sea level record: influence of glacial melting rates on the Younger Dryas event and deep-ocean circulation. *Nature*, vol. 342, pp. 637-642.
- Houmark-Nielsen M, Linge H, Fabel D, Schnabel C, Xue S, Wilcken KM, Binnie S (2012) Cosmogenic surface exposure dating the last deglaciation in Denmark: discrepancies with independent age constraints suggest delayed periglacial landform stabilisation. *Quat Geochronol* 13:1–17
- Jensen, J. B., og Bennike, O., 2020. General geology of southern MA, the Hesselø wind farm area. Report for Energinet Eltransmission A/S. Rapport 2020/53.
- Jensen, J. B., Bennike, O., and Vangkilde-Pedersen, T., 2023. Screening of seabed geological conditions for the offshore wind farm area Hesselø South and the adjacent cable corridor area. Desk study for Energinet. Rapport 2023/30. GEUS.
- Jensen J. B., Petersen K. S., Konradi P., Kuijpers A., Bennike O., Lemke W., Endler R., (2002) Neotectonics, sea-level changes and biological evolution in the Fennoscandian border zone of the southern Kattegat Sea. *Boreas* 31:133–150. doi:10.1111/j.1502-3885.2002.tb01062.x
- Lambeck, K., Rouby, H., Purcell, Y.S. & Sambridge, M. 2014: Sea-level and global ice volumes from the Last Glacial Maximum to the Holocene. *Proceedings of the National Academy of the United States of America (PNAS)* 111, 15296–15303.
- Reimer, P. et al. 2020. The IntCal20 Northern Hemisphere radiocarbon age calibration curve (0-55 cal kB. *Radiocarbon* 62, doi: 10.1017/RDC.2020.41.

Appendices:

Appendix 8.0 ARCHAEOLOGY CONFIDENCE 1 SSS-anomalies

Name	Desc	UClass1	UClass2	TLength	TWidth	Shadow	THeight	Latitude	Longitude
HS_B01_SSS_GO6_1888	ARCHAEOLOGY CONFIDENCE 1	Metallic DM	Medium	0,85	0,38	1,18	0,62	56,39878957	11,62949821
HS_B01_SSS_GO6_2207	ARCHAEOLOGY CONFIDENCE 1 Sonar Contact. Possible debris.	Other OD	High	0,66	0,46	0,57	0,19	56,39871991	11,62924581
HS_B01_SSS_GO6_2208	ARCHAEOLOGY CONFIDENCE 1 Sonar Contact. Possible debris.	Other OD	High	1,09	0,82	2,01	0,68	56,39872247	11,62927215
HS_B02_SSS_GO6_0037	Debris. Linear object. No clear shadow.	Other OD	Medium	10,83	0,24	0	0	56,40263809	11,73010951
HS_B02_SSS_GO6_0484	Debris. Possibly related with linear object.	Other OD	High	2,75	1	2,5	0,44	56,38058795	11,76312677
HS_B02_SSS_GO6_0485	Debris. Linear object.	Other OD	Medium	9,61	0,28	0,89	0,17	56,38059369	11,76317985
HS_B02_SSS_GO6_0496	Debris.	Other OD	Medium	0,67	0,25	0,39	0,14	56,38642819	11,75758014
HS_B02_SSS_GO6_0497	Debris.	Other OD	High	2,16	0,38	1,23	0,4	56,38643166	11,75760288
HS_B02_SSS_GO6_0525		Metallic DM	High	2,41	0,83	1,65	0,31	56,39432628	11,73101657
HS_B03_SSS_GO6_0105	Debris. Possibly related to the adjacent wreck.	Other OD	Medium	1,72	0,38	1,03	0,21	56,39377318	11,68351287
HS_B03_SSS_GO6_0104	Debris. Possibly related to the adjacent wreck.	Other OD	Medium	3,77	0,39	1,2	0,16	56,39364268	11,68336188
HS_B03_SSS_GO6_0106	Unknown shipwreck. UMINI	Wreck DW	High	31,61	10,77	13,7	3,63	56,39411084	11,6836062
HS_B04_SSS_GO6_0707	Debris. aNCHOR	Other OD	High	2,91	1,28	1,47	0,16	56,34965659	11,78397641

Appendix 8.1 ARCHAEOLOGY CONFIDENCE 2 SSS-anomalies

Name	Desc	UClass1	UClass2	TLength	TWidth	Shadow	THeight	Latitude	Longitude
HS_B01_SSS_GO 6_0328	ARCHAEOLOGY CONFIDENCE 2	Archaeology ARCH	High	0,87	0,24	1,37	0,5	56,30135878	11,52343743
HS_B01_SSS_GO 6_0581	ARCHAEOLOGY CONFIDENCE 2	Archaeology ARCH	High	0,55	0,22	1,02	0,4	56,30649684	11,52819578
HS_B01_SSS_GO 6_0584	ARCHAEOLOGY CONFIDENCE 2	Metallic DM	High	1,27	0,23	1,91	0,47	56,30664403	11,53338426
HS_B01_SSS_GO 6_0607	ARCHAEOLOGY CONFIDENCE 2	Metallic DM	High	2,3	0,76	5,72	0,27	56,30775809	11,53577143
HS_B01_SSS_GO 6_0615	ARCHAEOLOGY CONFIDENCE 2	Archaeology ARCH	High	1,18	0,58	1,03	1,79	56,30805961	11,53308128
HS_B01_SSS_GO 6_1011	ARCHAEOLOGY CONFIDENCE 2 Metallic DM	Archaeology ARCH	High	0,66	0,28	0,66	0,23	56,32605615	11,55084849
HS_B01_SSS_GO 6_1012	ARCHAEOLOGY CONFIDENCE 2 Boulder BD	Archaeology ARCH	High	0,72	0,34	0,86	0,32	56,32607477	11,55089744
HS_B01_SSS_GO 6_2003	ARCHAEOLOGY CONFIDENCE 2	Metallic DM	Medium	0,92	0,54	1,03	0,11	56,34538054	11,58149827
HS_B01_SSS_GO 6_2211	ARCHAEOLOGY CONFIDENCE 2 Boulder BD	Archaeology ARCH	High	0,59	0,27	0,76	0,2	56,32575007	11,55464446
HS_B01_SSS_GO 6_2212	ARCHAEOLOGY CONFIDENCE 2	Archaeology ARCH	High	0,95	0,23	0,95	0,29	56,32576222	11,55457756
HS_B01_SSS_GO 6_2291	ARCHAEOLOGY CONFIDENCE 2 Boulder BD	Archaeology ARCH	High	2,79	1,63	4,08	1,05	56,32623294	11,54820068
HS_B01_SSS_GO 6_2487	ARCHAEOLOGY CONFIDENCE 2 Boulder BD	Archaeology ARCH	High	2,33	1	2,43	0,5	56,29557816	11,52013986
HS_B01_SSS_GO 6_3089	ARCHAEOLOGY CONFIDENCE 2	Archaeology ARCH		0	0	0	0	56,35208117	11,58206549
HS_B01_SSS_GO 6_3094	ARCHAEOLOGY CONFIDENCE 2	Archaeology ARCH	Medium	0	0	0	0	56,36146247	11,58834083
HS_B01_SSS_GO 6_3099	ARCHAEOLOGY CONFIDENCE 2	Archaeology ARCH	High	0	0	0	0	56,3622962	11,58576814
HS_B01_SSS_GO 6_3101	ARCHAEOLOGY CONFIDENCE 2 more visible in mosaic, HS_B01_MBES_GO6_0561	Archaeology ARCH	High	0	0	0	0	56,29415881	11,5192839
HS_B03_SSS_GO 6_0025	Debris. Linear object.	Other OD	Medium	7,91	0,5	1,29	0,39	56,33183579	11,84455964
HS_B03_SSS_GO 6_0100	Debris. Elongated object.	Other OD	Medium	2,95	0,51	0,95	0,2	56,38992895	11,68861136
HS_B03_SSS_GO 6_0041	Debris. Possibly related with rope.	Other OD	High	4,15	0,23	0,64	0,13	56,33292259	11,84495285
HS_B03_SSS_GO 6_0042	Possible rope.	Soft Rope SR	High	8,32	0,73	0,88	0,22	56,33294242	11,84502125
HS_B04_SSS_GO 6_0386		Metallic DM	High	1,09	0,22	2,73	1,79	56,32871234	11,79407128
HS_B04_SSS_GO 6_0598		Metallic DM	High	0,98	0,76	1,73	0,88	56,3312304	11,81822529

MAV2023-050 Hesselø South

Name	Desc	UClass1	UClass2	TLength	TWidth	Shadow	THeight	Latitude	Longitude
HS_B04_SSS_GO 6_0791		Metallic DM	High	0,75	0,3	2,38	0,21	56,33241438	11,81789454
HS_B04_SSS_GO 6_0659	Debris.	Other OD	High	1,72	0,83	1,97	0,28	56,37550044	11,70653822
HS_B04_SSS_GO 6_0660	Debris.	Other OD	Medium	0,74	0,68	4,23	0,53	56,375504	11,70659433
HS_B04_SSS_GO 6_0714	Debris.	Other OD	High	1,07	0,7	1,66	0,16	56,33236489	11,82541007
HS_B05_SSS_GO 6_1633	Sonar Contact. Within 10 metres from MAG target HS_B05_MAG_GO6_0093. See rectangular object 55m to W	Other OD	Medium	0,84	0,49	1,84	0,12	56,33008706	11,7304875
HS_B05_SSS_GO 6_1692		Metallic DM	High	1,75	1,27	6,96	0,65	56,3300007	11,74218187
HS_B05_SSS_GO 6_1934	Sonar Contact. Within 10 metres from MAG target HS_B05_MAG_GO6_0267.	Other OD	High	1,25	0,72	3	0,24	56,34773327	11,68504094
HS_B08_SSS_GO 6_2921		Metallic DM	High	1,84	0,66	4,21	0,49	56,30116345	11,53386308
HS_B08_SSS_GO 6_2922		Metallic DM	High	1,59	0,64	9,81	0,85	56,30401974	11,57825142
HS_B08_SSS_GO 6_2923		Metallic DM	High	1,25	0,32	4,42	0,56	56,31278592	11,58732731
HS_B08_SSS_GO 6_2924		Metallic DM	High	3,02	0,97	16,98	1,44	56,31273552	11,58900242
HS_B08_SSS_GO 6_0408	Debris. Elongated object.	Other OD	High	4,62	0,25	2,16	0,23	56,29496644	11,60845229

Appendix 8.2 ARCHAEOLOGY CONFIDENCE 3 SSS-anomalies

Name	Desc	UClass1	UClass2	TLength	TWidth	Shadow	THeight	Latitude	Longitude
HS_B01_SSS_GO6_0007	ARCHAEOLOGY CONFIDENCE 3 Boulder BD	Archaeology ARCH	Medium	0,51	0,22	0,3	0,2	56,29371228	11,51814261
HS_B01_SSS_GO6_0011	ARCHAEOLOGY CONFIDENCE 3	Metallic DM	Medium	0,51	0,37	0,98	0,12	56,29384013	11,51993904
HS_B01_SSS_GO6_0016	ARCHAEOLOGY CONFIDENCE 3 Stretched MBES HS_B01_MBES_GO6_0567	Archaeology ARCH	High	2,18	0,51	3,7	0,4	56,29407055	11,5145774
HS_B01_SSS_GO6_0024	ARCHAEOLOGY CONFIDENCE 3 Boulder BD	Archaeology ARCH	High	0,81	0,47	0,79	0,25	56,2943006	11,51844423
HS_B01_SSS_GO6_0070	ARCHAEOLOGY CONFIDENCE 3 Close to nadir. metallic DM	Archaeology ARCH	High	1,75	0,9	1,51	2,36	56,29563136	11,51728163
HS_B01_SSS_GO6_0105	ARCHAEOLOGY CONFIDENCE 3	Metallic DM	High	0,54	0,17	1,22	0,29	56,29610344	11,52193001
HS_B01_SSS_GO6_0166	ARCHAEOLOGY CONFIDENCE 3	Archaeology ARCH	High	5,85	4,15	8,22	1,77	56,29683952	11,5183753
HS_B01_SSS_GO6_0192	ARCHAEOLOGY CONFIDENCE 3	Metallic DM	High	1,59	0,73	2,79	1,98	56,29746127	11,52233174
HS_B01_SSS_GO6_0269	ARCHAEOLOGY CONFIDENCE 3	Metallic DM	High	0,76	0,33	1,47	0,34	56,2999248	11,52647776

MAV2023-050 Hesselø South

Name	Desc	UClass1	UClass2	TLength	TWidth	Shadow	THeight	Latitude	Longitude
HS_B01_SSS_GO6_0275	ARCHAEOLOGY CONFIDENCE 3 BOULDER ?	Metallic DM	High	1,69	0,38	2,91	1,27	56,30012007	11,51979029
HS_B01_SSS_GO6_0311	ARCHAEOLOGY CONFIDENCE 3	Archaeology ARCH	High	0,8	0,28	1,85	0,91	56,30094594	11,52238172
HS_B01_SSS_GO6_0425	ARCHAEOLOGY CONFIDENCE 3 Sonar Contact. No mag anomaly.	Other OD	High	3,23	1,1	7,81	0,5	56,30254627	11,53119457
HS_B01_SSS_GO6_0465	ARCHAEOLOGY CONFIDENCE 3	Metallic DM	Low	0,8	0,31	1,03	0,1	56,30293352	11,53001411
HS_B01_SSS_GO6_0469	ARCHAEOLOGY CONFIDENCE 3	Archaeology ARCH	High	1,76	0,2	1,27	0,97	56,30298971	11,52436923
HS_B01_SSS_GO6_0476	ARCHAEOLOGY CONFIDENCE 3 Metallic DM	Archaeology ARCH	High	0,64	0,27	1,39	0,32	56,30307731	11,53019431
HS_B01_SSS_GO6_0487	ARCHAEOLOGY CONFIDENCE 3	Metallic DM	High	0,75	0,3	1,12	0,25	56,30317343	11,53031103
HS_B01_SSS_GO6_0508	ARCHAEOLOGY CONFIDENCE 3	Metallic DM	Medium	0,53	0,22	1,21	0,37	56,30349176	11,53061524
HS_B01_SSS_GO6_0519	ARCHAEOLOGY CONFIDENCE 3 Boulder BD	Archaeology ARCH	High	0,52	0,4	0,47	0,56	56,30377149	11,52393513
HS_B01_SSS_GO6_0533	ARCHAEOLOGY CONFIDENCE 3	Metallic DM	Medium	1,07	0,64	0,95	0,18	56,30418083	11,53042529

MAV2023-050 Hesselø South

Name	Desc	UClass1	UClass2	TLength	TWidth	Shadow	THeight	Latitude	Longitude
HS_B01_SSS_GO6_0572	ARCHAEOLOGY CONFIDENCE 3	Metallic DM	Medium	0,55	0,2	0,94	0,19	56,30599004	11,53257481
HS_B01_SSS_GO6_0575	ARCHAEOLOGY CONFIDENCE 3	Metallic DM	High	1,12	0,41	0,98	0,19	56,30604868	11,53262194
HS_B01_SSS_GO6_0596	ARCHAEOLOGY CONFIDENCE 3	Metallic DM	High	1,63	1,16	6,13	0,29	56,30698382	11,53483518
HS_B01_SSS_GO6_0612	ARCHAEOLOGY CONFIDENCE 3 Boulder BD	Archaeology ARCH	High	1,13	0,26	3,04	0,51	56,30793153	11,53446508
HS_B01_SSS_GO6_0622	ARCHAEOLOGY CONFIDENCE 3	Metallic DM	High	0,74	0,2	1,37	0,46	56,30992865	11,53838077
HS_B01_SSS_GO6_0626	ARCHAEOLOGY CONFIDENCE 3	Archaeology ARCH	High	0,55	0,24	0,81	0,36	56,31054797	11,53571797
HS_B01_SSS_GO6_0627	ARCHAEOLOGY CONFIDENCE 3	Metallic DM	High	0,55	0,4	0,93	0,25	56,3105545	11,53913274
HS_B01_SSS_GO6_0681	ARCHAEOLOGY CONFIDENCE 3	Archaeology ARCH	High	0,82	0,51	2,32	0,45	56,31411379	11,53955968
HS_B01_SSS_GO6_0694	ARCHAEOLOGY CONFIDENCE 3	Metallic DM	High	0,71	0,23	1,13	0,31	56,31442754	11,54258965
HS_B01_SSS_GO6_0728	ARCHAEOLOGY CONFIDENCE 3 Boulder BD	Archaeology ARCH	High	2,31	0,49	2,12	1,59	56,31568028	11,54321537
HS_B01_SSS_GO6_0747	ARCHAEOLOGY CONFIDENCE 3	Metallic DM	Medium	0,64	0,25	0,34	0,16	56,31608331	11,54468789
HS_B01_SSS_GO6_0803	ARCHAEOLOGY	Archaeology ARCH	High	1,75	0,91	6,47	0,95	56,31931153	11,54287853

MAV2023-050 Hesselø South

Name	Desc	UClass1	UClass2	TLength	TWidth	Shadow	THeight	Latitude	Longitude
	CONFIDEN CE 3 Boulder BD								
HS_B01_SSS_GO6_0863	ARCHAEO LOGY CONFIDEN CE 3 Boulder BD	Archaeology ARCH	High	0,89	0,69	0,9	0,34	56,32116972	11,54158432
HS_B01_SSS_GO6_0918	ARCHAEO LOGY CONFIDEN CE 3 Debris. Elongated object.	Other OD	Medium	5,01	0,41	0,79	0,1	56,32291491	11,55519798
HS_B01_SSS_GO6_0986	ARCHAEO LOGY CONFIDEN CE 3	Archaeology ARCH	High	1,57	0,49	3,46	0,61	56,32534119	11,55212689
HS_B01_SSS_GO6_1058	ARCHAEO LOGY CONFIDEN CE 3	Archaeology ARCH	High	1,05	0,26	0,63	0,35	56,33053175	11,55695255
HS_B01_SSS_GO6_1063	ARCHAEO LOGY CONFIDEN CE 3 Boulder BD	Archaeology ARCH	High	0,85	0,61	1,36	0,33	56,33274776	11,55826952
HS_B01_SSS_GO6_1064	ARCHAEO LOGY CONFIDEN CE 3 Linear debris. Possible cable/rope fragment.	Soft Rope SR	Medium	19,29	0,2	0,62	0,09	56,33486373	11,56954134
HS_B01_SSS_GO6_1070	ARCHAEO LOGY CONFIDEN CE 3 Boulder BD	Archaeology ARCH	High	1,37	0,72	2,84	0,45	56,34379553	11,57158101
HS_B01_SSS_GO6_1109	ARCHAEO LOGY CONFIDEN CE 3	Archaeology ARCH	High	1,33	0,35	2,54	0,55	56,35123641	11,57308974
HS_B01_SSS_GO6_1206	ARCHAEO LOGY CONFIDEN	Archaeology ARCH	High	1,63	0,74	3,75	0,48	56,35666394	11,58349815

MAV2023-050 Hesselø South

Name	Desc	UClass1	UClass2	TLength	TWidth	Shadow	THeight	Latitude	Longitude
	CE 3 Boulder BD								
HS_B01_SSS_GO6_1344	ARCHAEO LOGY CONFIDEN CE 3 Boulder BD	Archaeology ARCH	High	0,77	0,71	0,94	0,26	56,36072337	11,58792008
HS_B01_SSS_GO6_1898	ARCHAEO LOGY CONFIDEN CE 3 Debris.	Other OD	High	4,32	0,8	1,42	0,16	56,42737955	11,66626828
HS_B01_SSS_GO6_1899	ARCHAEO LOGY CONFIDEN CE 3 No clear shadow. Scouring.	Metallic DM	Medium	0,61	0,49	0,25	0,09	56,35961249	11,58869631
HS_B01_SSS_GO6_1906	ARCHAEO LOGY CONFIDEN CE 3	Archaeology ARCH	Medium	1,12	0,44	0,96	0,15	56,32286961	11,54966655
HS_B01_SSS_GO6_1908	ARCHAEO LOGY CONFIDEN CE 3 Debris. other OD	Archaeology ARCH	High	3,1	1,71	2,85	1,5	56,30187241	11,52416577
HS_B01_SSS_GO6_1910	ARCHAEO LOGY CONFIDEN CE 3 Sonar Contact.	Other OD	High	1,81	0,93	6,6	1,05	56,32386461	11,54997923
HS_B01_SSS_GO6_1911	ARCHAEO LOGY CONFIDEN CE 3 Sonar Contact.	Other OD	High	2,56	1,08	7,42	0,79	56,31978959	11,54517096
HS_B01_SSS_GO6_1918	ARCHAEO LOGY CONFIDEN CE 3 Debris.	Other OD	High	4,42	2,38	3,33	1,96	56,30075392	11,52479432
HS_B01_SSS_GO6_1920	ARCHAEO LOGY CONFIDEN CE 3 Debris.	Other OD	High	3	1,51	3,73	0,36	56,29625346	11,51985126

MAV2023-050 Hesselø South

Name	Desc	UClass1	UClass2	TLength	TWidth	Shadow	THeight	Latitude	Longitude
HS_B01_SSS_GO6_2004	ARCHAEOLOGY CONFIDENCE 3	Metallic DM	Medium	1,78	0,96	1,8	0,57	56,35108288	11,58135484
HS_B01_SSS_GO6_2005	ARCHAEOLOGY CONFIDENCE 3	Metallic DM	High	1,26	0,59	0,8	0,08	56,35157252	11,57431434
HS_B01_SSS_GO6_2027	ARCHAEOLOGY CONFIDENCE 3 Boulder BD	Archaeology ARCH	Medium	0,59	0,19	0,6	0,25	56,33097783	11,55326231
HS_B01_SSS_GO6_2032	ARCHAEOLOGY CONFIDENCE 3 Boulder BD	Archaeology ARCH	Medium	0,51	0,34	0,74	0,27	56,33139742	11,5570606
HS_B01_SSS_GO6_2377	ARCHAEOLOGY CONFIDENCE 3	Archaeology ARCH	High	2,95	1,5	6,86	0,98	56,34860529	11,58120044
HS_B01_SSS_GO6_2470	ARCHAEOLOGY CONFIDENCE 3 Boulder BD	Archaeology ARCH	High	2,09	1,18	2,72	0,88	56,30234568	11,52522873
HS_B01_SSS_GO6_2588	ARCHAEOLOGY CONFIDENCE 3 Boulder BD	Archaeology ARCH	High	2,56	1,23	2,73	1,02	56,30202074	11,52508188
HS_B01_SSS_GO6_3088	ARCHAEOLOGY CONFIDENCE 3	Archaeology ARCH	Medium	0	0	0	0	56,3666425	11,5904534
HS_B01_SSS_GO6_3090	ARCHAEOLOGY CONFIDENCE 3	Archaeology ARCH		0	0	0	0	56,31880318	11,54333977
HS_B01_SSS_GO6_3091	ARCHAEOLOGY CONFIDENCE 3	Archaeology ARCH		0	0	0	0	56,29899595	11,52217198
HS_B01_SSS_GO6_3092	ARCHAEOLOGY CONFIDENCE 3	Archaeology ARCH	Low	0	0	0	0	56,35494181	11,57638966

MAV2023-050 Hesselø South

Name	Desc	UClass1	UClass2	TLength	TWidth	Shadow	THeight	Latitude	Longitude
	CE 3 boulder?								
HS_B01_SSS_GO6_3093	ARCHAEOLOGY CONFIDENCE 3	Archaeology ARCH	Medium	0	0	0	0	56,33432347	11,55272651
HS_B01_SSS_GO6_3098	ARCHAEOLOGY CONFIDENCE 3	Archaeology ARCH	Low	0	0	0	0	56,34882026	11,56997038
HS_B01_SSS_GO6_3100	ARCHAEOLOGY CONFIDENCE 3	Archaeology ARCH	Medium	0	0	0	0	56,36490184	11,58994481
HS_B02_SSS_GO6_0290	Sonar Contact.	Other OD	Medium	0,68	0,71	1,1	0,13	56,33667694	11,90304223
HS_B02_SSS_GO6_0471		Metallic DM	High	0,52	0,29	0,55	0,21	56,34394105	11,8931594
HS_B02_SSS_GO6_0472	Sonar contact at 6m from HS_B02_MAG_GO6_019.	Other OD	High	0,9	0,74	0,76	0,29	56,34395526	11,89312502
HS_B03_SSS_GO6_0112		Metallic DM	High	1,22	0,44	5,16	2,09	56,33318179	11,85096706
HS_B04_SSS_GO6_0541	Linear object.	Metallic DM	High	49,64	0,53	1,74	0,17	56,32880414	11,79690454
HS_B04_SSS_GO6_0730		Metallic DM	High	2,68	0,7	1,2	0,56	56,38528824	11,68756347
HS_B04_SSS_GO6_0790	Maybe CONF2 check 75m to SE, possibly geology	Metallic DM	High	1,84	0,88	2,08	1,61	56,33204465	11,82824513
HS_B04_SSS_GO6_0160	Debris.	Other OD	High	3,11	1,66	11,19	1,08	56,32866833	11,79702451
HS_B04_SSS_GO6_0239	Debris.	Other OD	High	1,17	0,47	0,72	0,93	56,32902143	11,80408325
HS_B04_SSS_GO6_0542	Debris.	Other OD	Medium	1,37	0,3	1,12	0,16	56,33505987	11,79145066
HS_B04_SSS_GO6_0546	Debris. Intense scouring.	Other OD	High	1,36	0,56	1,78	0,3	56,34134528	11,78216104
HS_B04_SSS_GO6_0563	Debris.	Other OD	High	0,97	0,53	2,08	0,26	56,33047308	11,81830068

MAV2023-050 Hesselø South

Name	Desc	UClass1	UClass2	TLength	TWidth	Shadow	THeight	Latitude	Longitude
HS_B04_SSS_GO6_0564	Debris.	Other OD	High	1,15	0,56	1,6	0,18	56,33048774	11,81838012
HS_B04_SSS_GO6_0622	Debris.	Other OD	High	1,24	0,7	2,56	0,23	56,33111783	11,82135947
HS_B04_SSS_GO6_0634	Debris.	Other OD	Medium	0,74	0,44	1,35	0,15	56,33201058	11,82324882
HS_B04_SSS_GO6_0786	Possible debris.	Other OD	High	5,06	1,03	2,61	0,3	56,37369165	11,68102748
HS_B04_SSS_GO6_0825	Sonar Contact. Within 10 metres from MAG target HS_B04_M AG_GO6_045.	Other OD	Low	0,82	0,33	1,11	0,16	56,33172235	11,78858795
HS_B05_SSS_GO6_0016	Debris.	Other OD	High	2,58	0,92	0,44	0,2	56,33366053	11,76894152
HS_B05_SSS_GO6_0519	Sonar Contact. Within 10 metres from MAG target HS_B05_M AG_GO6_078.	Other OD	High	1,77	1,07	9,55	0,74	56,32951432	11,73229741
HS_B05_SSS_GO6_0682	Possible rope/wire fragment.	Other OD	Medium	34,55	0,17	0,76	0,08	56,32658534	11,74285293
HS_B05_SSS_GO6_0704		Metallic DM	High	1	0,38	1,76	0,24	56,33666872	11,71527119
HS_B05_SSS_GO6_0934	Possible rope/wire/cable fragment.	Other OD	Medium	27,45	0,67	2,7	0,38	56,32609703	11,74771512
HS_B05_SSS_GO6_1014	Debris.	Other OD	High	2,44	1,19	2,45	0,81	56,34092709	11,71277622
HS_B05_SSS_GO6_1015	Debris.	Other OD	High	2,72	0,91	1,41	0,45	56,34094937	11,71276952
HS_B05_SSS_GO6_1282	Debris.	Other OD	High	2,95	2,2	0,65	0,12	56,3494301	11,6681222
HS_B05_SSS_GO6_1366		Metallic DM	High	1,9	1,06	3,21	0,28	56,33422235	11,71059853
HS_B05_SSS_GO6_1374	Possible rope/wire/cable fragment.	Other OD	High	40,38	0,75	0,45	0,05	56,34840023	11,67462352

MAV2023-050 Hesselø South

Name	Desc	UClass1	UClass2	TLength	TWidth	Shadow	THeight	Latitude	Longitude
HS_B05_SSS_GO6_1400	Debris.	Other OD	High	3,02	1,44	1,24	0,34	56,33309913	11,74199946
HS_B05_SSS_GO6_1465	Debris. Elongated object.	Other OD	Medium	3,03	0,3	0,33	0,07	56,35565563	11,69069389
HS_B05_SSS_GO6_1533	Debris.	Other OD	High	1,71	0,54	3,64	0,48	56,32771326	11,77469147
HS_B05_SSS_GO6_1545	Debris.	Other OD	High	3,53	1,63	0,3	0,09	56,3533878	11,70322484
HS_B05_SSS_GO6_1547	Sonar Contact. Elongated objects. Two more nearby objects with similar characteristics.	Other OD	Low	2,43	0,59	1,39	0,15	56,35741896	11,69402131
HS_B05_SSS_GO6_1548	Sonar Contact. Elongated objects. Two more nearby objects with similar characteristics.	Other OD	High	1,94	1,19	0,61	0,08	56,35740085	11,69381452
HS_B05_SSS_GO6_1549	Sonar Contact. Elongated objects. Two more nearby objects with similar characteristics.	Other OD	High	1,38	0,43	0,18	0,03	56,35740884	11,69364681
HS_B05_SSS_GO6_1567	Debris.	Other OD	High	3,41	2,83	0,58	0,1	56,35914702	11,69021361
HS_B05_SSS_GO6_1569	Sonar Contact. Within 10 metres from MAG target HS_B05_MAG_GO6_0230.	Other OD	High	2,23	1,92	2,58	0,36	56,33711585	11,75151195

MAV2023-050 Hesselø South

Name	Desc	UClass1	UClass2	TLength	TWidth	Shadow	THeight	Latitude	Longitude
HS_B05_SSS_GO6_1587	Possible rope/wire fragment.	Soft Rope SR	Medium	63,03	0,27	0,97	0,07	56,32725683	11,74730342
HS_B05_SSS_GO6_1619	Possible rope/wire fragment.	Soft Rope SR	Medium	39,25	0,88	0,27	0,05	56,32545935	11,74238721
HS_B05_SSS_GO6_1694		Metallic DM	High	3,01	2,8	8,96	0,87	56,32721872	11,75449848
HS_B05_SSS_GO6_1695		Metallic DM	High	1,53	1,01	5,63	0,57	56,32719043	11,75453273
HS_B05_SSS_GO6_1697		Metallic DM	High	2,44	1,38	3,31	1,09	56,32935546	11,72529932
HS_B05_SSS_GO6_1701		Metallic DM	High	2,76	1,68	6,88	0,56	56,34451917	11,69697254
HS_B05_SSS_GO6_1705		Metallic DM	High	2,13	0,68	7,24	0,74	56,34468588	11,68199323
HS_B05_SSS_GO6_1706		Metallic DM	High	1,77	1,72	5,81	0,62	56,34470833	11,68197123
HS_B05_SSS_GO6_1712		Metallic DM	High	1,59	0,82	1,21	0,12	56,33382175	11,71732483
HS_B05_SSS_GO6_1717	Debris. Possible linear object attached.	Other OD	High	2,37	1,31	5,1	0,51	56,32554435	11,74266411
HS_B05_SSS_GO6_1718	Debris. Possible wire/rope attached.	Other OD	High	2,07	1,55	3,77	0,41	56,32654027	11,74294496
HS_B05_SSS_GO6_1720	Sonar Contact.	Other OD	High	3,49	2,25	9,79	0,8	56,32715279	11,75439301
HS_B05_SSS_GO6_1767		Metallic DM	High	1,41	0,48	5,51	0,56	56,32728864	11,7542378
HS_B05_SSS_GO6_1781		Metallic DM	High	0,65	0,36	2,21	0,22	56,32775211	11,77488991
HS_B05_SSS_GO6_1782		Metallic DM	High	1,51	0,68	3,87	0,38	56,32779744	11,77477788
HS_B05_SSS_GO6_1878	Sonar Contact. Within 10 metres from MAG target HS_B05_M AG_GO6_0 260.	Other OD	High	1,01	0,68	2,62	0,21	56,3458612	11,69028849
HS_B05_SSS_GO6_1880	Sonar Contact. Within 10	Other OD	Medium	0,65	0,28	0,78	0,08	56,32706398	11,73865113

MAV2023-050 Hesselø South

Name	Desc	UClass1	UClass2	TLength	TWidth	Shadow	THeight	Latitude	Longitude
	metres from MAG target HS_B05_M AG_GO6_0 023.								
HS_B05_SSS_GO6_1881	Sonar Contact. Within 10 metres from MAG target HS_B05_M AG_GO6_0 026.	Other OD	High	0,65	0,48	2,47	0,34	56,32733135	11,73721993
HS_B05_SSS_GO6_1882	Sonar Contact. Within 10 metres from MAG target HS_B05_M AG_GO6_0 036.	Other OD	High	1,04	0,48	1,32	0,49	56,32789794	11,73669997
HS_B05_SSS_GO6_1884	Sonar Contact. Within 10 metres from MAG target HS_B05_M AG_GO6_0 047.	Other OD	High	1,3	0,74	4,44	0,38	56,32761476	11,76521336
HS_B05_SSS_GO6_1888	Sonar Contact. Within 10 metres from MAG target HS_B05_M AG_GO6_0 076.	Other OD	High	0,58	0,27	0,42	0,22	56,32835973	11,77897366
HS_B05_SSS_GO6_1891	Sonar Contact. Within 10 metres from MAG target HS_B05_M AG_GO6_0 099.	Other OD	Medium	0,51	0,32	0,36	0,2	56,33017926	11,73045702
HS_B05_SSS_GO6_1892	Sonar Contact. Within 10 metres from	Other OD	Medium	0,52	0,24	0,27	0,18	56,32932467	11,77641924

MAV2023-050 Hesselø South

Name	Desc	UClass1	UClass2	TLength	TWidth	Shadow	THeight	Latitude	Longitude
	MAG target HS_B05_M AG_GO6_0 105.								
HS_B05_SSS_GO6_1899	Sonar Contact. Within 10 metres from MAG target HS_B05_M AG_GO6_0 128.	Other OD	High	0,78	0,24	0,45	0,27	56,33129697	11,71855861
HS_B05_SSS_GO6_1928	Sonar Contact. Within 10 metres from MAG target HS_B05_M AG_GO6_0 242.	Other OD	High	0,59	0,18	1,22	0,33	56,34227837	11,70198331
HS_B05_SSS_GO6_1935		Metallic DM	High	1,06	0,73	6,19	0,73	56,34830966	11,67482054
HS_B05_SSS_GO6_1937	Sonar Contact. Within 10 metres from MAG target HS_B05_M AG_GO6_0 277.	Other OD	Medium	0,95	0,87	1,76	0,16	56,34887799	11,68205876
HS_B06_SSS_GO6_2182	Debris. Elongated contact.	Other OD	Medium	1,68	0,37	0,36	0,06	56,33012544	11,67572021
HS_B06_SSS_GO6_3574	Sonar Contact.	Other OD	Medium	0,65	0,25	0,4	0,09	56,33638103	11,67574144
HS_B06_SSS_GO6_3575	Sonar Contact.	Other OD	Medium	1,59	0,51	0,91	0,2	56,33606817	11,67662236
HS_B06_SSS_GO6_3689	Sonar Contact.	Other OD	High	1,68	0,76	0,65	0,12	56,33293425	11,68397888
HS_B06_SSS_GO6_4693	Sonar Contact.	Other OD	Medium	0,9	0,34	0,78	0,13	56,33728364	11,68782331
HS_B06_SSS_GO6_5549	Debris.	Other OD	Medium	1,02	0,18	0,45	0,05	56,32841364	11,71917196
HS_B06_SSS_GO6_5602	Sonar Contact. Stretched.	Other OD	Medium	1,84	0,33	0,42	0,04	56,34137994	11,68931768
HS_B06_SSS_GO6_5787	Debris.	Other OD	High	2,62	0,71	0,53	0,16	56,31981103	11,67673243

MAV2023-050 Hesselø South

Name	Desc	UClass1	UClass2	TLength	TWidth	Shadow	THeight	Latitude	Longitude
HS_B06_SSS_GO6_5801	Sonar Contact.	Other OD	Low	1,41	0,2	0,38	0,08	56,32176952	11,6643817
HS_B07_SSS_GO6_0176		Metallic DM	High	1,72	1,04	1,68	1,25	56,31054029	11,66171114
HS_B07_SSS_GO6_0092		Metallic DM	High	3,36	0,67	1,35	0,25	56,30748874	11,62240428
HS_B07_SSS_GO6_0783		Metallic DM	High	0,52	0,29	0,25	0,05	56,32133344	11,61015961
HS_B07_SSS_GO6_0468		Metallic DM	High	1,08	0,47	2,72	0,47	56,31605941	11,61096808
HS_B07_SSS_GO6_0356		Metallic DM	High	2,37	1,7	6,06	1,25	56,31375517	11,59021684
HS_B07_SSS_GO6_0930		Metallic DM	High	1,43	0,82	6,16	0,86	56,30250239	11,62052054
HS_B07_SSS_GO6_0931	Unclear object.	Metallic DM	Medium	0,77	0,52	0,64	0,08	56,3057796	11,61141219
HS_B07_SSS_GO6_0932		Metallic DM	Medium	0,58	0,35	1,33	0,18	56,3204843	11,63663358
HS_B07_SSS_GO6_0575	Sonar Contact.	Other OD	Medium	1,36	0,56	1,38	0,43	56,31716342	11,65717119
HS_B07_SSS_GO6_0572	Sonar Contact. Cluster of unknown objects.	Other OD	Medium	1,59	0,53	1,2	0,34	56,31714761	11,65713032
HS_B07_SSS_GO6_0566	Sonar Contact. Cluster of unknown objects.	Other OD	Medium	0,94	0,74	1,11	0,29	56,31712118	11,657129
HS_B07_SSS_GO6_0573	Sonar Contact. Cluster of unknown objects.	Other OD	Medium	1,7	1,29	1,84	0,46	56,31714888	11,65705784
HS_B07_SSS_GO6_0560	Sonar Contact. Cluster of unknown objects.	Other OD	Medium	2,09	1,43	1,23	0,26	56,31707789	11,6570642
HS_B07_SSS_GO6_0565	Sonar Contact. Cluster of unknown objects.	Other OD	Medium	1,62	0,71	1,05	0,23	56,31711683	11,65700424
HS_B07_SSS_GO6_0556	Sonar Contact. Cluster of	Other OD	Medium	2,29	1,41	1,84	0,34	56,31706066	11,65700626

MAV2023-050 Hesselø South

Name	Desc	UClass1	UClass2	TLength	TWidth	Shadow	THeight	Latitude	Longitude
	unknown objects.								
HS_B07_SSS_GO6_0558	Sonar Contact. Cluster of unknown objects.	Other OD	Medium	0,9	0,88	1,49	0,27	56,31707191	11,65694049
HS_B07_SSS_GO6_0586	Sonar Contact. Cluster of unknown objects.	Other OD	Medium	2,22	1,64	3,47	0,37	56,31728624	11,65740793
HS_B07_SSS_GO6_0580	Sonar Contact. Cluster of unknown objects.	Other OD	Medium	2,32	1,21	1,78	0,19	56,3172351	11,65754549
HS_B07_SSS_GO6_0577	Sonar Contact. Cluster of unknown objects.	Other OD	Medium	1,85	0,93	2,52	0,35	56,31719669	11,6572563
HS_B07_SSS_GO6_0199	Debris.	Other OD	High	2,08	1,24	1,47	0,55	56,31129218	11,659269
HS_B07_SSS_GO6_0164	Debris.	Other OD	High	2,66	0,64	1,05	0,2	56,3101512	11,62661282
HS_B07_SSS_GO6_0040	Sonar Contact.	Other OD	High	0,69	0,57	1,62	0,35	56,30579076	11,61115877
HS_B07_SSS_GO6_0933	Debris. Possible rope attached.	Other OD	High	1,76	0,83	3,8	1,33	56,30961065	11,62047094
HS_B07_SSS_GO6_0141		Soft Rope SR	High	22,19	0,41	0,67	0,07	56,30949056	11,62049539
HS_B08_SSS_GO6_0252		Metallic DM	High	2,59	1,44	1,67	2,01	56,29433023	11,53036564
HS_B08_SSS_GO6_0837	Close to nadir.	Metallic DM	High	1,47	1,09	1,19	1,72	56,29659612	11,52725136
HS_B08_SSS_GO6_1796		Metallic DM	High	2,22	0,78	1,44	0,57	56,30300383	11,53212773
HS_B08_SSS_GO6_2917		Metallic DM	High	2,42	0,43	5,05	0,61	56,29388415	11,53644802
HS_B08_SSS_GO6_2918		Metallic DM	High	0,84	0,41	0,89	0,52	56,29400425	11,53412416
HS_B08_SSS_GO6_2919		Metallic DM	High	0,57	0,15	0,76	0,51	56,29417765	11,53367174
HS_B08_SSS_GO6_2920		Metallic DM	High	0,5	0,3	1,98	0,94	56,29494046	11,53914256

MAV2023-050 Hesselø South

Name	Desc	UClass1	UClass2	TLength	TWidth	Shadow	THeight	Latitude	Longitude
HS_B08_SSS_GO6_3014		Metallic DM	High	2,04	1,25	3,21	0,67	56,29815912	11,52636558
HS_B08_SSS_GO6_4516		Metallic DM	High	1,53	0,7	2,69	0,58	56,31690679	11,5486146
HS_B08_SSS_GO6_4517		Metallic DM	High	1,64	1,11	2,36	0,33	56,31718197	11,5489563
HS_B08_SSS_GO6_4523		Metallic DM	High	1,19	0,84	1,32	0,44	56,29994963	11,52846281
HS_B08_SSS_GO6_4525	Unclear object.	Metallic DM	Medium	1,04	0,57	0,99	0,37	56,2984871	11,52666105
HS_B08_SSS_GO6_4527		Metallic DM	High	1,15	0,51	1,29	0,29	56,2975842	11,52564211
HS_B08_SSS_GO6_4533		Metallic DM	High	0,88	0,49	1,33	0,28	56,31693033	11,54862029
HS_B08_SSS_GO6_4540		Metallic DM	Medium	0,98	0,74	2,27	0,22	56,31720259	11,54887685
HS_B08_SSS_GO6_0149	Sonar Contact. Within 10 metres from MAG target HS_B08_M AG_GO6_0001.	Other OD	High	0,74	0,45	1,34	0,14	56,29400897	11,52513625
HS_B08_SSS_GO6_0715	Debris.	Other OD	High	1,66	0,45	3,06	0,8	56,29608577	11,52447354
HS_B08_SSS_GO6_0745	Sonar Contact. Within 10 metres from MAG target HS_B08_M AG_GO6_0007.	Other OD	High	1,05	0,38	2,05	0,28	56,29617968	11,52994849
HS_B08_SSS_GO6_1197	Sonar Contact. Within 10 metres from MAG target HS_B01_M AG_GO6_0086	Other OD	High	1,01	0,94	3,51	0,57	56,29857294	11,52686245
HS_B08_SSS_GO6_1168	Sonar Contact. Within 10 metres from MAG target HS_B01_M	Other OD	High	0,69	1,16	1,21	1,75	56,29841622	11,52654199

MAV2023-050 Hesselø South

Name	Desc	UClass1	UClass2	TLength	TWidth	Shadow	THeight	Latitude	Longitude
	AG_GO6_0089								
HS_B08_SSS_GO6_2256	Debris. Possible unclear linear object attached.	Other OD	High	1,43	0,29	1,77	0,71	56,30669989	11,56364085
HS_B08_SSS_GO6_1254	Sonar Contact. Within 10 metres from MAG target HS_B01_M AG_GO6_0084	Other OD	High	1,05	0,53	0,67	0,16	56,29889347	11,52710254
HS_B08_SSS_GO6_1216	Sonar Contact. Within 10 metres from MAG target HS_B01_M AG_GO6_0086	Other OD	High	0,65	0,27	0,94	0,49	56,29865685	11,52699009
HS_B08_SSS_GO6_1819	Sonar Contact. Within 10 metres from MAG target HS_B01_M AG_GO6_0078.	Other OD	Medium	0,95	0,16	0,69	0,13	56,3031597	11,53220752
HS_B08_SSS_GO6_1784	Sonar Contact. Within 10 metres from MAG target HS_B01_M AG_GO6_0079	Other OD	High	0,84	0,16	0,78	0,63	56,30293744	11,53208852
HS_B08_SSS_GO6_1548	Debris. Rectangular shape.	Other OD	High	3,52	3,04	13,21	1,51	56,30177181	11,59057964
HS_B08_SSS_GO6_4518	Sonar Contact. Within 10 metres from MAG target HS_B01_M	Other OD	High	1,82	1,15	5,7	0,63	56,31712179	11,54886619

MAV2023-050 Hesselø South

Name	Desc	UClass1	UClass2	TLength	TWidth	Shadow	THeight	Latitude	Longitude
	AG_GO6_0069.								
HS_B08_SSS_GO6_4519	Sonar Contact. Within 10 metres from MAG target HS_B01_M AG_GO6_0070	Other OD	High	1,22	0,55	1,36	0,33	56,31687193	11,54864697
HS_B08_SSS_GO6_4520	Sonar Contact. Within 10 metres from MAG target HS_B01_M AG_GO6_0070	Other OD	High	1,2	0,94	2,06	0,45	56,31687539	11,54870165
HS_B08_SSS_GO6_4521	Sonar Contact. Within 10 metres from MAG target HS_B01_M AG_GO6_0073	Other OD	High	0,6	0,39	1,06	0,15	56,31398289	11,54524042
HS_B08_SSS_GO6_4524	Sonar Contact. Within 10 metres from MAG target HS_B01_M AG_GO6_0082	Other OD	High	1,11	0,53	0,96	0,86	56,2998302	11,52845278
HS_B08_SSS_GO6_4526	Sonar Contact. Within 10 metres from MAG target HS_B01_M AG_GO6_0090	Other OD	High	1,32	0,7	2,1	0,52	56,29811227	11,52638221
HS_B08_SSS_GO6_4528	Sonar Contact. Within 10 metres from MAG target HS_B01_M	Other OD	High	1,09	0,5	1,46	0,37	56,29765223	11,52553163

MAV2023-050 Hesselø South

Name	Desc	UClass1	UClass2	TLength	TWidth	Shadow	THeight	Latitude	Longitude
	AG_GO6_0091								
HS_B08_SSS_GO6_4532	Sonar Contact. Within 10 metres from MAG target HS_B01_M AG_GO6_0069	Other OD	High	0,97	0,46	1,88	0,25	56,31720295	11,54883837
HS_B08_SSS_GO6_4534		Other OD	High	0,9	0,48	1,2	0,23	56,31698057	11,5485458
HS_B08_SSS_GO6_4538	Sonar Contact. Within 10 metres from MAG target HS_B01_M AG_GO6_0070	Other OD	High	1,53	0,69	4,3	0,43	56,31683959	11,54852735
HS_B08_SSS_GO6_4539	Sonar Contact. Within 10 metres from MAG target HS_B01_M AG_GO6_0070	Other OD	High	0,91	0,45	1,22	0,33	56,31689127	11,54849074

Appendix 8.3 ARCHAEOLOGY CONFIDENCE 4 SSS-anomalies

Name	Desc	UClass1	UClas s2	TLengt h	TWidt h	Shado w	THeig ht	Latitude	Longitude
HS_B01_SSS_GO6_0620	ARCHAEOLOGY CONFIDENCE 4 Debris.	Other OD	High	3,35	1,16	21,39	1,39	56,308482 47	11,536019 95
HS_B01_SSS_GO6_0806	ARCHAEOLOGY CONFIDENCE 4 Debris.	Archaeology ARCH	High	4,18	0,88	15,56	2,81	56,319682 7	11,541603 64
HS_B01_SSS_GO6_1372	ARCHAEOLOGY CONFIDENCE 4	Metallic DM	High	1,5	0,59	1,21	0,41	56,361059 61	11,585547 35
HS_B01_SSS_GO6_1395	ARCHAEOLOGY CONFIDENCE 4 Debris. Possible tyre, rounded object.	Other OD	High	0,71	0,52	0,67	0,55	56,361352 27	11,590768 85
HS_B01_SSS_GO6_1418	ARCHAEOLOGY CONFIDENCE 4 Linear object, linear debris.	Soft Rope SR	Mediu m	13,9	0,19	0,5	0,06	56,361541 92	11,588734 87
HS_B01_SSS_GO6_1424	ARCHAEOLOGY CONFIDENCE 4 Debris. Possible rope/cable fragments attached.	Other OD	Mediu m	1,27	0,67	0,74	0,1	56,361599	11,588793 43
HS_B01_SSS_GO6_1900	ARCHAEOLOGY CONFIDENCE 4 Sonar Contact. Elongated object.	Other OD	Mediu m	1,35	0,39	1,17	0,4	56,301455 98	11,528534 35
HS_B01_SSS_GO6_1937	ARCHAEOLOGY CONFIDENCE 4 Sonar Contact.	Other OD	High	1,67	0,62	2,62	0,43	56,299919 91	11,520567 12
HS_B01_SSS_GO6_3096	ARCHAEOLOGY CONFIDENCE 4	Archaeology ARCH	Low	0	0	0	0	56,427280 56	11,666472 08
HS_B01_SSS_GO6_3097	ARCHAEOLOGY CONFIDENCE 4	Archaeology ARCH	Mediu m	0	0	0	0	56,344682 76	11,565025 42
HS_B02_SSS_GO6_0269	Debris.	Other OD	High	2,7	0,27	1,76	0,64	56,336178 58	11,903227 78
HS_B02_SSS_GO6_0492	Linear object. No shadow clear.	Metallic DM	Mediu m	16,06	2,9	0	0	56,383727 93	11,761413 49
HS_B02_SSS_GO6_0522	Sonar contact possibly related to the adjacent wreck.	Other OD	Mediu m	0,61	0,49	0,34	0,1	56,416539 5	11,690693 42
HS_B02_SSS_GO6_0523	Unknown shipwreck. S/S CIMBRIA	Wreck DW	High	29,24	6,89	27,99	3,09	56,416759 96	11,690423 23
HS_B02_SSS_GO6_0524		Metallic DM	Mediu m	0,68	0,45	0,92	0,1	56,417003 36	11,690960 99
HS_B05_SSS_GO6_0291	Unknown shipwreck. BORINGIA	Wreck DW	High	30,43	6,77	32,8	2,1	56,382284 01	11,642095 07
HS_B05_SSS_GO6_1551	Linear object. Possible rope.	Soft Rope SR	High	10,6	0,31	0,51	0,08	56,367376 56	11,666619 7
HS_B05_SSS_GO6_1584	Linear object. Possible rope.	Soft Rope SR	High	14,36	0,46	0,21	0,05	56,361860 08	11,688421 7
HS_B05_SSS_GO6_1648	Possible debris. Related to fishing activities.	Other OD	High	7,33	1,98	1,77	0,47	56,370127 13	11,629317
HS_B07_SSS_GO6_0717	Sonar Contact. Cluster of unknown objects.	Other OD	Mediu m	1,83	0,65	1,7	0,36	56,319160 95	11,660786 62
HS_B07_SSS_GO6_0605	Sonar Contact. Cluster of unknown objects.	Other OD	Mediu m	1,47	1,09	1,79	0,32	56,317579 73	11,657677 1
HS_B07_SSS_GO6_0602	Sonar Contact. Cluster of unknown objects.	Other OD	Mediu m	3,39	1,67	2,17	0,37	56,317545 44	11,657812 6

MAV2023-050 Hesselø South

Name	Desc	UClass1	UClass2	TLengh	TWidh	Shadow	THeight	Latitude	Longitude
HS_B07_SSS_GO6_0616	Sonar Contact. Cluster of unknown objects.	Other OD	Medium	2,62	1,45	2,75	0,34	56,31771741	11,65773714
HS_B07_SSS_GO6_0614	Sonar Contact. Cluster of unknown objects.	Other OD	Medium	2,11	1,58	2,81	0,31	56,3176834	11,65801272
HS_B07_SSS_GO6_0603	Sonar Contact.	Other OD	Medium	1,4	0,91	0,85	0,25	56,31754841	11,65738236
HS_B07_SSS_GO6_0748	Sonar Contact. Cluster of unknown objects.	Other OD	Medium	1,98	1,03	3,22	0,39	56,31999052	11,6590889
HS_B07_SSS_GO6_0742	Sonar Contact. Cluster of unknown objects.	Other OD	Medium	1,29	0,66	1,17	0,21	56,31976711	11,65921096
HS_B07_SSS_GO6_0736	Sonar Contact. Cluster of unknown objects.	Other OD	Medium	0,85	0,67	0,94	0,21	56,31964732	11,65930541
HS_B07_SSS_GO6_0739	Sonar Contact. Cluster of unknown objects.	Other OD	Medium	1,55	1,09	2,02	0,3	56,31971078	11,65955569
HS_B07_SSS_GO6_0741	Sonar Contact. Cluster of unknown objects.	Other OD	Medium	1,24	0,53	0,88	0,15	56,31973971	11,65935125
HS_B07_SSS_GO6_0744	Sonar Contact. Cluster of unknown objects.	Other OD	Medium	0,82	0,5	1,11	0,17	56,3198246	11,65927069
HS_B07_SSS_GO6_0743	Sonar Contact. Cluster of unknown objects.	Other OD	Medium	1,65	1,02	1,26	0,19	56,31982024	11,65933802
HS_B07_SSS_GO6_0735	Sonar Contact. Cluster of unknown objects.	Other OD	Medium	1,13	0,59	2,52	0,31	56,319634	11,66000181
HS_B07_SSS_GO6_0731	Sonar Contact. Cluster of unknown objects.	Other OD	Medium	1,47	1,15	2,37	0,3	56,31956546	11,66012574
HS_B07_SSS_GO6_0737	Sonar Contact. Cluster of unknown objects.	Other OD	Medium	1,79	0,65	1,01	0,11	56,31967331	11,66005567
HS_B07_SSS_GO6_0728	Sonar Contact. Cluster of unknown objects.	Other OD	Medium	0,98	1,5	1,78	0,28	56,31943043	11,6602042
HS_B07_SSS_GO6_0700	Sonar Contact. Cluster of unknown objects.	Other OD	Medium	1,32	0,73	1,67	0,4	56,31900745	11,65952082
HS_B07_SSS_GO6_0691	Sonar Contact. Cluster of unknown objects.	Other OD	Medium	1	0,41	0,95	0,15	56,31886493	11,6595149
HS_B07_SSS_GO6_0683	Sonar Contact. Cluster of unknown objects.	Other OD	Medium	2,99	1,14	0,32	0,03	56,31877477	11,65909098
HS_B07_SSS_GO6_0689	Sonar Contact. Cluster of unknown objects.	Other OD	Medium	1,63	0,62	2,58	0,32	56,31885008	11,65921679
HS_B07_SSS_GO6_0694	Sonar Contact. Cluster of unknown objects.	Other OD	Medium	1,12	0,61	1,35	0,19	56,31893893	11,65911779
HS_B07_SSS_GO6_0693	Sonar Contact. Cluster of unknown objects.	Other OD	Medium	1,04	0,77	1,93	0,27	56,31892599	11,65921202
HS_B07_SSS_GO6_0698	Sonar Contact. Cluster of unknown objects.	Other OD	Medium	1,68	0,41	1,73	0,3	56,31899965	11,65925591
HS_B07_SSS_GO6_0703	Sonar Contact. Cluster of unknown objects.	Other OD	Medium	1,4	0,54	1,58	0,36	56,31904134	11,65938693
HS_B07_SSS_GO6_0707	Sonar Contact. Cluster of unknown objects.	Other OD	Medium	0,99	0,47	1,17	0,31	56,31906785	11,65939121

MAV2023-050 Hesselø South

Name	Desc	UClass1	UClass2	TLengh	TWidh	Shadow	THeight	Latitude	Longitude
HS_B07_SSS_GO6_0711	Sonar Contact. Cluster of unknown objects.	Other OD	Medium	0,83	0,74	1,26	0,36	56,3190855	11,65940943
HS_B07_SSS_GO6_0712	Sonar Contact. Cluster of unknown objects.	Other OD	Medium	1,91	0,79	1,02	0,32	56,31909898	11,65942939
HS_B07_SSS_GO6_0531	Sonar Contact.	Other OD	Medium	1,83	1,44	3,48	0,39	56,31673367	11,65696184
HS_B07_SSS_GO6_0949	Sonar Contact. Cluster of unknown objects.	Other OD	Medium	0,85	0,36	0,98	0,17	56,31942592	11,66014638
HS_B07_SSS_GO6_0950	Sonar Contact. Cluster of unknown objects.	Other OD	Medium	0,96	0,44	1,06	0,22	56,31949106	11,6597943
HS_B07_SSS_GO6_0952	Sonar Contact. Cluster of unknown objects.	Other OD	Medium	0,94	0,73	1,68	0,25	56,31961705	11,65981333
HS_B07_SSS_GO6_0951	Sonar Contact. Cluster of unknown objects.	Other OD	Medium	1,79	1,66	3,34	0,37	56,3195839	11,66028204
HS_B07_SSS_GO6_0945	Sonar Contact. Cluster of unknown objects.	Other OD	Medium	0,97	0,41	2,31	0,43	56,31860893	11,66044915
HS_B07_SSS_GO6_0944	Sonar Contact. Cluster of unknown objects.	Other OD	Medium	0,86	0,35	1,1	0,17	56,31860149	11,66024629
HS_B07_SSS_GO6_0942	Sonar Contact. Cluster of unknown objects.	Other OD	Medium	1,11	0,39	2,54	0,29	56,31841836	11,66033613
HS_B07_SSS_GO6_0943	Sonar Contact. Cluster of unknown objects.	Other OD	Medium	0,99	0,47	1,1	0,13	56,31849953	11,66016562
HS_B07_SSS_GO6_0948	Sonar Contact. Cluster of unknown objects.	Other OD	Medium	0,82	0,38	0,85	0,32	56,31918591	11,65928205
HS_B07_SSS_GO6_0947	Sonar Contact. Cluster of unknown objects.	Other OD	Medium	0,76	0,48	0,79	0,48	56,31917485	11,65950176
HS_B07_SSS_GO6_0946	Sonar Contact. Cluster of unknown objects.	Other OD	Medium	0,7	0,43	0,88	0,25	56,31896123	11,65976681
HS_B07_SSS_GO6_0934	Sonar Contact. Cluster of unknown objects.	Other OD	Medium	0,83	0,76	2,39	0,38	56,31689065	11,65732904
HS_B07_SSS_GO6_0939	Sonar Contact. Cluster of unknown objects.	Other OD	Medium	1,33	0,97	2,02	0,28	56,317008	11,65678922
HS_B07_SSS_GO6_0938	Sonar Contact. Cluster of unknown objects.	Other OD	Medium	1,19	0,7	1,87	0,24	56,31697804	11,65676944
HS_B07_SSS_GO6_0937	Sonar Contact. Cluster of unknown objects.	Other OD	Medium	1,26	0,6	2,15	0,25	56,31694706	11,65670809
HS_B07_SSS_GO6_0936	Sonar Contact. Cluster of unknown objects.	Other OD	Medium	1,04	0,78	1,47	0,17	56,31693085	11,65667701
HS_B07_SSS_GO6_0935	Sonar Contact. Cluster of unknown objects.	Other OD	Medium	1	0,53	2,21	0,23	56,31690032	11,65659074
HS_B07_SSS_GO6_0941	Sonar Contact. Cluster of unknown objects.	Other OD	Medium	2,08	0,79	2,4	0,31	56,31747515	11,65846709
HS_B07_SSS_GO6_0940	Sonar Contact. Cluster of unknown objects.	Other OD	Medium	1,35	0,55	2,23	0,3	56,31742694	11,65853776

Appendix 8.4 MAG-anomalies

Target ID	X	Y	Comment	P2P	Interpretation
HS_B01_MAG_G06_0001	655949,5	6241643,5	not enough data to calculate depths and weights	43,84	positive monopole
HS_B01_MAG_G06_0008	656025,3	6241832,5	not enough data to calculate depths and weights, 1	133,31	complex
HS_B01_MAG_G06_0009	655781	6241831,5	not enough data to calculate depths and weights, 1	45,62	diapole
HS_B01_MAG_G06_0047	656554	6242810	not enough data to calculate depths and weights, 1	137,27	diapole
HS_B01_MAG_G06_0050	656680	6243016,5	not enough data to calculate depths and weights, 1	41,88	positive monopole
HS_B01_MAG_G06_0056	656449	6243103	not enough data to calculate depths and weights, 1	121,09	positive monopole
HS_B01_MAG_G06_0082	657729	6245292	not enough data to calculate depths and weights	42,93	positive monopole
HS_B01_MAG_G06_0086	659515,5	6248148,5	not enough data to calculate depths and weights	60,12	positive monopole
HS_B01_MAG_G06_0093	660595	6250704	not enough data to calculate depths and weights	174,34	diapole
HS_B01_MAG_G06_0094	660605,5	6250721	not enough data to calculate depths and weights	91,9	diapole
HS_B01_MAG_G06_0095	661687,5	6252365	not enough data to calculate depths and weights	59,41	diapole
HS_B01_MAG_G06_0099	662283	6253566,5	not enough data to calculate depths and weights	45,08	diapole
HS_B01_MAG_G06_0100	662944	6254661	not enough data to calculate depths and weights	59,37	diapole
HS_B02_MAG_G06_0001	678876,87	6247839,04		39,4	Dipole
HS_B02_MAG_G06_0004	671930,87	6251605,54	not enough data to calculate Eulers depths and wei	51,5	Monopole positive
HS_B02_MAG_G06_0005	665994,37	6255743,54	Possible wreck related	14,7	Monopole negative
HS_B02_MAG_G06_0006	678107,5	6247289		45	Complex
HS_B02_MAG_G06_0007	678055	6247321		43,7	Complex
HS_B02_MAG_G06_0008	678330	6247378	not enough data to calculate Eulers depths and wei	55,1	Monopole positive
HS_B02_MAG_G06_0009	677668,5	6247412,5		44,8	Monopole positive
HS_B02_MAG_G06_0010	678009,5	6247481,5	not enough data to calculate Eulers depths and wei	61,5	Monopole positive
HS_B02_MAG_G06_0012	677641,5	6247507	not enough data to calculate Eulers depths and wei	62,9	Complex

MAV2023-050 Hesselø South

HS_B02_MAG_G06_00 14	678852,5	6247798	not enough data to calculate Eulers depths and wei	66,4	Monopole positive
HS_B02_MAG_G06_00 15	678918	6247813,5	not enough data to calculate Eulers depths and wei	42,2	Monopole positive
HS_B02_MAG_G06_00 18	678962,5	6247927,5	not enough data to calculate Eulers depths and wei	261,9	Monopole negative
HS_B02_MAG_G06_00 19	678809	6248120,5	not enough data to calculate Eulers depths and wei	58	Monopole positive
HS_B02_MAG_G06_00 27	668562,5	6253312,5	not enough data to calculate Eulers depths and wei	75,2	Monopole positive
HS_B02_MAG_G06_00 30	665932	6255690,5	Possible wreck related	37	Dipole
HS_B02_MAG_G06_00 32	678143,74 06	6247489,6 47	not enough data to calculate Eulers depths and wei	68,2	Monopole positive
HS_B02_MAG_G06_00 33	678210,04 92	6247448,8 77	not enough data to calculate Eulers depths and wei	83,1	Monopole positive
HS_B02_MAG_G06_00 43	677597	6247310	weight < 50 kg	54,1	Dipole
HS_B02_MAG_G06_00 49	677709,5	6247660	weight < 50 kg	45,8	Complex
HS_B03_MAG_G06_00 06	676688	6247062		40,1	Positive monopole
HS_B03_MAG_G06_00 14	672871	6248646	not enough data to calculate Eulers depths and weights	197,1	Positive monopole
HS_B03_MAG_G06_00 17	669640	6251344		54,3	Negative monopole
HS_B03_MAG_G06_00 19	665642,5	6253184,5	not enough data to calculate Eulers depths and weights. Strong anomaly.	733,6	Negative monopole
HS_B03_MAG_G06_00 28	666569	6252330	weight < 50 kg	49,5	Positive monopole
HS_B04_MAG_G06_00 29	667201,8	6250791,5	not enough data to calculate Eulers depths and weights	42,45	Diapole
HS_B04_MAG_G06_00 16	672093	6248102	not enough data to calculate Eulers depths and weights	62,19	Diapole
HS_B04_MAG_G06_00 49	662954,5	6253400	not enough data to calculate Eulers depths and weights	43,88	Diapole
HS_B04_MAG_G06_00 43	663522,5	6252315	not enough data to calculate Eulers depths and weights	342,07	Diapole
HS_B04_MAG_G06_00 42	665924	6252205,5	not enough data to calculate Eulers depths and weights	52,55	Diapole
HS_B04_MAG_G06_00 38	665949,5	6251603,5	not enough data to calculate Eulers depths and weights	50,21	Diapole
HS_B04_MAG_G06_00 35	666078,8	6251230,8	not enough data to calculate Eulers depths and weights	81,12	Diapole
HS_B05_MAG_G06_00 10	670444,5	6245703,5	not enough data to calculate Euler depths and weights	185,28	Positive monopole
HS_B05_MAG_G06_00 58	669675,5	6245944,5	not enough data to calculate Eulers depths and weights	147,21	Negative monopole

MAV2023-050 Hesselø South

HS_B05_MAG_G06_00 69	669113,5	6245987,5	not enough data to calculate Eulers depths and weights	62,36	Positive monopole
HS_B05_MAG_G06_00 72	669093	6246000,5		62,93	Positive monopole
HS_B05_MAG_G06_00 91	668497,5	6246073,5	not enough data to calculate Eulers depths and weights	46,47	Positive monopole
HS_B05_MAG_G06_00 98	668921	6246103,5	not enough data to calculate Eulers depths and weights	81,65	Diapole
HS_B05_MAG_G06_00 123	669538,5	6246185	not enough data to calculate Eulers depths and weights	67,89	Diapole
HS_B05_MAG_G06_00 126	670518	6246195,5	not enough data to calculate Eulers depths and weights	129,66	Negative monopole
HS_B05_MAG_G06_00 129	670506,5	6246203	not enough data to calculate Eulers depths and weights	78,29	Diapole
HS_B05_MAG_G06_00 160	670269,5	6246340		70,39	Positive monopole
HS_B05_MAG_G06_00 180	670188	6246386,5		116,15	Positive monopole
HS_B05_MAG_G06_00 189	670125,5	6246419		72,98	Positive monopole
HS_B05_MAG_G06_00 198	670037,5	6246471		60,73	Positive monopole
HS_B05_MAG_G06_00 216	667988	6246548,5	not enough data to calculate Eulers depths and weights	50,56	Positive monopole
HS_B05_MAG_G06_00 223	667570,5	6246576		68,28	Positive monopole
HS_B05_MAG_G06_00 236	669635,5	6246715	not enough data to calculate Eulers depths and weights	68,28	Positive monopole
HS_B05_MAG_G06_00 242	669146,5	6246851	not enough data to calculate Eulers depths and weights	42,91	Positive monopole
HS_B05_MAG_G06_00 243	667846,5	6246860,5	not enough data to calculate Eulers depths and weights	47,89	Positive monopole
HS_B05_MAG_G06_00 244	669172,5	6246885	not enough data to calculate Eulers depths and weights	79,02	Positive monopole
HS_B05_MAG_G06_00 245	667143,5	6246894,5		71,39	Positive monopole
HS_B05_MAG_G06_00 247	669172,5	6246957,5	not enough data to calculate Eulers depths and weights	61,34	Positive monopole
HS_B05_MAG_G06_00 249	669183,8	6246993	not enough data to calculate Eulers depths and weights	90,15	Positive monopole
HS_B05_MAG_G06_00 253	666867,5	6247103,5		59,9	Diapole
HS_B05_MAG_G06_00 259	667005,5	6247373		42,11	Positive monopole
HS_B05_MAG_G06_00 272	665755	6247672		40,02	Positive monopole (target 272)
HS_B05_MAG_G06_00 273	665752	6247673,5		40,02	Positive monopole

MAV2023-050 Hesselø South

HS_B05_MAG_G06_00 274	666685	6247686,5		42,24	Positive monopole
HS_B05_MAG_G06_00 283	667961	6247955	not enough data to calculate Eulers depths and weights	70,01	Diapole
HS_B05_MAG_G06_00 289	668520,5	6248057		138,66	Diapole
HS_B05_MAG_G06_00 300	669013	6248199		89,37	Diapole
HS_B05_MAG_G06_00 308	667217,5	6248779		78,93	Negative monopole
HS_B05_MAG_G06_00 312	663334,5	6249134	not enough data to calculate Eulers depths and weights	137,24	Diapole
HS_B05_MAG_G06_00 314	666395	6249152	not enough data to calculate Eulers depths and weights, SFSwreck 1928	118,71	Negative monopole
HS_B05_MAG_G06_00 316	664990	6249295		47,31	Diapole
HS_B05_MAG_G06_00 320	664490	6249442,5	not enough data to calculate Eulers depths and weights	87,96	Diapole
HS_B05_MAG_G06_00 321	663319	6249466,5	not enough data to calculate Eulers depths and weights	122,89	Diapole
HS_B05_MAG_G06_00 322	662857	6249543,5		72,86	Diapole
HS_B05_MAG_G06_00 324	664434	6249877	not enough data to calculate Eulers depths and weights	77,49	Negative monopole
HS_B05_MAG_G06_00 326	665303,5	6250005		88,7	Diapole
HS_B05_MAG_G06_00 331	663812	6250325		45,25	Negative monopole
HS_B05_MAG_G06_00 332	664759,5	6250388,5	not enough data to calculate Eulers depths and weights	91,53	Diapole
HS_B05_MAG_G06_00 334	661566	6250673,5		45,26	Diapole
HS_B05_MAG_G06_00 336	663130,8	6251768,8	not enough data to calculate Eulers depths and weights	3485,5 8	Negative monopole
HS_B06_MAG_GO6_0 001	666542,5	6245731			
HS_B06_MAG_GO6_0 002	665019,5	6245930			
HS_B06_MAG_GO6_0 003	668327,5	6246060,5			
HS_B06_MAG_GO6_0 004	667850,5	6246164			
HS_B06_MAG_GO6_0 005	667459,5	6246181			
HS_B06_MAG_GO6_0 006	667725	6246322			
HS_B06_MAG_GO6_0 007	667002,5	6246456,5			

MAV2023-050 Hesselø South

HS_B06_MAG_GO6_0 008	666908,5	6246558,5		
HS_B06_MAG_GO6_0 009	667053,5	6246615		
HS_B06_MAG_GO6_0 010	666710,5	6246622		
HS_B06_MAG_GO6_0 011	667010,5	6246671,5		
HS_B06_MAG_GO6_0 012	665483,5	6246735,5		
HS_B06_MAG_GO6_0 013	666999,5	6246754,5		
HS_B06_MAG_GO6_0 014	666480	6246991		
HS_B06_MAG_GO6_0 015	661864,5	6247061		
HS_B06_MAG_GO6_0 016	666655	6247074,5		
HS_B06_MAG_GO6_0 017	664596	6247090		
HS_B06_MAG_GO6_0 018	662469,5	6247134		
HS_B06_MAG_GO6_0 019	661008,5	6247134,5		
HS_B06_MAG_GO6_0 020	665073	6247157,5		
HS_B06_MAG_GO6_0 021	661067	6247166,5		
HS_B06_MAG_GO6_0 022	662557	6247222,5		
HS_B06_MAG_GO6_0 023	661569	6247242,5		
HS_B06_MAG_GO6_0 024	662433	6247299		
HS_B06_MAG_GO6_0 025	665372	6247300		
HS_B06_MAG_GO6_0 026	661718,5	6247366,5		
HS_B06_MAG_GO6_0 027	662564	6247367,5		
HS_B06_MAG_GO6_0 028	662275,5	6247394		
HS_B06_MAG_GO6_0 029	662608,5	6247400,5		
HS_B06_MAG_GO6_0 030	661117,5	6247423		
HS_B06_MAG_GO6_0 031	665118	6247455		

MAV2023-050 Hesselø South

HS_B06_MAG_GO6_0 032	661274,5	6247479,5		
HS_B06_MAG_GO6_0 033	665069	6247483,5		
HS_B06_MAG_GO6_0 034	665492,5	6247485		
HS_B06_MAG_GO6_0 035	662330	6247508		
HS_B06_MAG_GO6_0 036	660851	6247520		
HS_B06_MAG_GO6_0 037	660712,5	6247521		
HS_B06_MAG_GO6_0 038	661169	6247541		
HS_B06_MAG_GO6_0 039	662625	6247542		
HS_B06_MAG_GO6_0 040	661288,5	6247557		
HS_B06_MAG_GO6_0 041	662458,5	6247579,5		
HS_B06_MAG_GO6_0 042	663951,5	6247597,5		
HS_B06_MAG_GO6_0 043	665800	6247600,5		
HS_B06_MAG_GO6_0 044	664123,5	6247603,5		
HS_B06_MAG_GO6_0 045	665174,5	6247607,5		
HS_B06_MAG_GO6_0 046	664407,5	6247623,5		
HS_B06_MAG_GO6_0 047	661275	6247629		
HS_B06_MAG_GO6_0 048	665539,5	6247643		
HS_B06_MAG_GO6_0 049	661620	6247647		
HS_B06_MAG_GO6_0 050	662101,5	6247648		
HS_B06_MAG_GO6_0 051	660620	6247659,5		
HS_B06_MAG_GO6_0 052	665031,5	6247660,5		
HS_B06_MAG_GO6_0 053	663913	6247690		
HS_B06_MAG_GO6_0 054	661637	6247702		
HS_B06_MAG_GO6_0 055	664119	6247730		

MAV2023-050 Hesselø South

HS_B06_MAG_GO6_0 056	662665,5	6247741,5		
HS_B06_MAG_GO6_0 057	661169	6247782,5		
HS_B06_MAG_GO6_0 058	664399,5	6247785		
HS_B06_MAG_GO6_0 059	664865	6247793,5		
HS_B06_MAG_GO6_0 060	663918	6247804		
HS_B06_MAG_GO6_0 061	661576	6247823,5		
HS_B06_MAG_GO6_0 062	660842	6247825,5		
HS_B06_MAG_GO6_0 063	661309,5	6247837		
HS_B06_MAG_GO6_0 064	665376	6247850,5		
HS_B06_MAG_GO6_0 065	665179,5	6247862,5		
HS_B06_MAG_GO6_0 066	665234,5	6247863,5		
HS_B06_MAG_GO6_0 067	661033,5	6247864,5		
HS_B06_MAG_GO6_0 068	664262	6247864,5		
HS_B06_MAG_GO6_0 069	665031	6247869		
HS_B06_MAG_GO6_0 070	664635,5	6247877		
HS_B06_MAG_GO6_0 071	665200,5	6247884		
HS_B06_MAG_GO6_0 072	660078,5	6247904,5		
HS_B06_MAG_GO6_0 073	664382,5	6247905		
HS_B06_MAG_GO6_0 074	664771,5	6247917		
HS_B06_MAG_GO6_0 075	664461	6247923		
HS_B06_MAG_GO6_0 076	662442	6247923,5		
HS_B06_MAG_GO6_0 077	661152,5	6247937		
HS_B06_MAG_GO6_0 078	664302	6247952,5		
HS_B06_MAG_GO6_0 079	664960,5	6247995		

MAV2023-050 Hesselø South

HS_B06_MAG_GO6_0 080	664770,5	6247996		
HS_B06_MAG_GO6_0 081	661485,5	6248017		
HS_B06_MAG_GO6_0 082	664275,5	6248042		
HS_B06_MAG_GO6_0 083	664934	6248042		
HS_B06_MAG_GO6_0 084	664648	6248107,5		
HS_B06_MAG_GO6_0 085	660545,5	6248159		
HS_B06_MAG_GO6_0 086	659998,5	6248248,5		
HS_B06_MAG_GO6_0 087	663137,5	6248328		
HS_B06_MAG_GO6_0 088	663155	6248608,5		
HS_B06_MAG_GO6_0 089	661316	6249190,5		
HS_B06_MAG_GO6_0 090	660826,5	6250428		
HS_B06_MAG_GO6_0 091	660830,57	6247161,0 4		
HS_B06_MAG_GO6_0 092	661067,87	6247303,1 9		
HS_B06_MAG_GO6_0 093	662476,23	6247420,0 3		
HS_B06_MAG_GO6_0 094	665019,5	6247697,7 9		
HS_B06_MAG_GO6_0 095	660372,57	6247809,1 3		
HS_B06_MAG_GO6_0 096	664478,5	6247350		
HS_B06_MAG_GO6_0 097	660642	6247355		
HS_B06_MAG_GO6_0 098	666006,5	6247360		
HS_B06_MAG_GO6_0 099	665586,5	6247361		
HS_B06_MAG_GO6_0 100	665580	6247364,5		
HS_B06_MAG_GO6_0 101	665847,5	6247570		
HS_B06_MAG_GO6_0 102	665229,5	6247579		
HS_B06_MAG_GO6_0 103	665517	6247581		

MAV2023-050 Hesselø South

HS_B06_MAG_GO6_0 104	664533,5	6247588		
HS_B06_MAG_GO6_0 105	662428	6247597,5		
HS_B06_MAG_GO6_0 106	664877	6247597,5		
HS_B06_MAG_GO6_0 107	664507	6247605,5		
HS_B06_MAG_GO6_0 108	664098,5	6247620		
HS_B06_MAG_GO6_0 109	664934,5	6247634		
HS_B06_MAG_GO6_0 110	664077	6247634,5		
HS_B06_MAG_GO6_0 111	664718	6247657,5		
HS_B06_MAG_GO6_0 112	665697,5	6247658		
HS_B06_MAG_GO6_0 113	665215,5	6247659,5		
HS_B06_MAG_GO6_0 114	665074	6247662		
HS_B06_MAG_GO6_0 115	664151	6247663,5		
HS_B06_MAG_GO6_0 116	665226,5	6247729		
HS_B06_MAG_GO6_0 117	665371	6247749		
HS_B06_MAG_GO6_0 118	664868	6247753,5		
HS_B06_MAG_GO6_0 119	664615	6247763,5		
HS_B06_MAG_GO6_0 120	665517	6247763,5		
HS_B06_MAG_GO6_0 121	665026,5	6247768,5		
HS_B06_MAG_GO6_0 122	664902	6247769,5		
HS_B06_MAG_GO6_0 123	664417,5	6247773,5		
HS_B06_MAG_GO6_0 124	664324	6247780		
HS_B06_MAG_GO6_0 125	664759	6247809,5		
HS_B06_MAG_GO6_0 126	664330,5	6247825		
HS_B06_MAG_GO6_0 127	663252	6247826		

MAV2023-050 Hesselø South

HS_B06_MAG_GO6_0 128	664123	6247834,5		
HS_B06_MAG_GO6_0 129	664653,5	6247864,5		
HS_B06_MAG_GO6_0 130	664750	6247871		
HS_B06_MAG_GO6_0 131	664043,5	6247881		
HS_B06_MAG_GO6_0 132	664212	6247894		
HS_B06_MAG_GO6_0 133	664399,5	6247895		
HS_B06_MAG_GO6_0 134	664019,5	6247895,5		
HS_B06_MAG_GO6_0 135	664489,5	6247902		
HS_B06_MAG_GO6_0 136	664184,5	6247911		
HS_B06_MAG_GO6_0 137	665285,5	6247911,5		
HS_B06_MAG_GO6_0 138	664586,5	6247912		
HS_B06_MAG_GO6_0 139	664272,5	6247927,5		
HS_B06_MAG_GO6_0 140	664344	6247927,5		
HS_B06_MAG_GO6_0 141	665258,5	6247930,5		
HS_B06_MAG_GO6_0 142	664659	6247934,5		
HS_B06_MAG_GO6_0 143	665052	6247939,5		
HS_B06_MAG_GO6_0 144	664322,5	6247940,5		
HS_B06_MAG_GO6_0 145	665234,5	6247950		
HS_B06_MAG_GO6_0 146	665225	6247958,5		
HS_B06_MAG_GO6_0 147	665216	6247965,5		
HS_B06_MAG_GO6_0 148	660614,5	6247967,5		
HS_B06_MAG_GO6_0 149	664273,5	6247969		
HS_B06_MAG_GO6_0 150	664356	6247989,5		
HS_B06_MAG_GO6_0 151	664463	6247992,5		

MAV2023-050 Hesselø South

HS_B06_MAG_GO6_0 152	664322,5	6248010,5		
HS_B06_MAG_GO6_0 153	664595	6248030,5		
HS_B06_MAG_GO6_0 154	664290	6248032,5		
HS_B06_MAG_GO6_0 155	664572,5	6248045,5		
HS_B06_MAG_GO6_0 156	664364	6248056		
HS_B06_MAG_GO6_0 157	664652	6248061,5		
HS_B06_MAG_GO6_0 158	664422,5	6248064		
HS_B06_MAG_GO6_0 159	664541	6248065,5		
HS_B06_MAG_GO6_0 160	661254,5	6248078		
HS_B06_MAG_GO6_0 161	664511	6248083,5		
HS_B06_MAG_GO6_0 162	664391	6248084		
HS_B06_MAG_GO6_0 163	664792	6248094,5		
HS_B06_MAG_GO6_0 164	664666	6248096,5		
HS_B06_MAG_GO6_0 165	664744	6248123		
HS_B06_MAG_GO6_0 166	664713	6248142		
HS_B06_MAG_GO6_0 167	664902,5	6248143		
HS_B06_MAG_GO6_0 168	664701	6248149,5		
HS_B06_MAG_GO6_0 169	664739	6248234		
HS_B06_MAG_GO6_0 170	664067	6248282,5		
HS_B06_MAG_GO6_0 171	662891	6248310,5		
HS_B06_MAG_GO6_0 172	663932	6248316		
HS_B06_MAG_GO6_0 173	663534	6248417,5		
HS_B06_MAG_GO6_0 174	663843	6248483,5		
HS_B06_MAG_GO6_0 175	664014,5	6248487,5		

MAV2023-050 Hesselø South

HS_B06_MAG_GO6_0 176	662335	6248531,5			
HS_B06_MAG_GO6_0 177	664131,5	6248606,5			
HS_B06_MAG_GO6_0 178	662396,5	6248719			
HS_B06_MAG_GO6_0 179	663513,5	6248752			
HS_B06_MAG_GO6_0 180	663372,5	6248769,5			
HS_B06_MAG_GO6_0 181	663460,5	6249020,5			
HS_B06_MAG_GO6_0 182	662879	6249070,5			
HS_B06_MAG_GO6_0 183	661419,5	6249233			
HS_B06_MAG_GO6_0 184	660972	6249290			
HS_B06_MAG_GO6_0 185	662168	6249727			
HS_B07_MAG_GO6_0 05	664648	6243823	not enough data to calculate depths and weights, burial depth calculated from Batch modeling	39,62	Positive monopole
HS_B07_MAG_GO6_0 03	662230	6243388	not enough data to calculate depths and weights, burial depth calculated from Batch modeling	56,71	Positive monopole
HS_B07_MAG_GO6_0 13	661578,5	6244891,5	170 fiducials, "not enough data to calculate depths and weights ", burial depth calculated from Batch modeling	74,66	Diapole
HS_B07_MAG_GO6_0 14	661418,7	6244902,8	"not enough data to calculate depths and weights ", burial depth calculated from Batch modeling	102,62	Complex
HS_B07_MAG_GO6_0 11	661502,5	6244851	not enough data to calculate depths and weights, burial depth calculated from Batch modeling	86,48	Complex
HS_B07_MAG_GO6_0 07	660214,5	6244012,5	not enough data to calculate depths and weights, burial depth calculated from Batch modeling	19,89	Positive monopole
HS_B08_MAG_GO6_0 001	656265,5	6241674,5	not enough data to calculate Euler's depths and weights	34,73	Positive monopole
HS_B08_MAG_GO6_0 004	656591,5	6241715		56,75	Diapole
HS_B08_MAG_GO6_0 007	656389,5	6241958,5	not enough data to calculate Euler's depths and weights	50,26	Positive monopole
HS_B08_MAG_GO6_0 008	656782,5	6242483	not enough data to calculate Euler's depths and weights	44,08	Diapole
HS_B08_MAG_GO6_0 009	659513,5	6242902,5	not enough data to calculate Euler's depths and weights	47,18	Diapole

Appendix 8.5 Borehole data

ID	Type	EUREF89 UTMX Z32 [m]	EUREF89 UTMY Z32 [m]	MSL EMODNET 2018
KG_1	CPT	647662	6256461	-21,31
KG_2	CPT + BH	646015	6254949	-22,32
KG_3	Optional	643200	6253881	-20,46
KG_4	CPT	646360	6253747	-35,56
KG_5	CPT	645069	6253169	-20,4
KG_6	CPT	641844	6252291	-21,09
KG_7	CPT + BH	640263	6251790	-20,94
KG_8	Optional	638051	6251572	-19,2
KG_9	CPT	644121	6251382	-21,5
KG_10	CPT	638149	6250456	-20,13
KG_11	CPT	635465	6250434	-19,63
KG_12	SCPT +BH	643644	6249431	-19,34
KG_13	CPT	640952	6249387	-34,21
KG_14	CPT	638929	6249088	-22,81
KG_15	CPT + BH	636246	6248943	-19,14
KG_16	Optional	642349	6248839	-18,42
KG_17	CPT	634511	6248632	-19,05
KG_18	Optional	636380	6247919	-20,15
KG_19	CPT	634502	6246495	-20,33
KG_20	CPT	637425	6246451	-25,6
KG_21	CPT + BH	636012	6244849	-26,41
KG_22	CPT	634021	6244538	-22,11
KG_23	CPT	636234	6242624	-21,57
KG_24	CPT	634489	6242258	-23,58
KG_25	SCPT + BH	634465	6240088	-20,49
KG_26	CPT	634236	6238035	-20,16

MAV2023-050 Hesselø South

ID	Type	EUREF89 UTMX Z32 [m]	EUREF89 UTMY Z32 [m]	MSL EMODNET 2018
KG_27	Optional	633759	6236058	-19,68
HS_S_1	CPT	664773	6256003	-27,57
HS_S_2	CPT + BH	665304	6254508	-26,91
HS_S_3	CPT	663622	6253191	-27,61
HS_S_4	CPT	667652	6253075	-25,46
HS_S_5	Optional	665850	6253003	-26,66
HS_S_6	SCPT + BH	670307	6252626	-24,92
HS_S_7	CPT	666183	6251628	-25,96
HS_S_8	Optional	668838	6251180	-24,69
HS_S_9	Optional	671493	6250731	-25,64
HS_S_10	CPT	662059	6250630	-24,86
HS_S_11	SCPT + BH	664074	6250572	-28,47
HS_S_12	CPT	673721	6250543	-28,22
HS_S_13	CPT	670118	6250398	-22,93
HS_S_14	CPT	667195	6249839	-24,02
HS_S_15	Optional	660580	6249190	-23,99
HS_S_16	Optional	662819	6248995	-26,48
HS_S_17	CPT	665035	6248787	-25,82
HS_S_18	CPT + BH	674719	6248819	-28,53
HS_S_19	Optional	669077	6248691	-21,61
HS_S_20	CPT	671305	6248503	-25,63
HS_S_21	CPT + BH	667702	6248358	-23,5
HS_S_22	CPT + BH	660713	6248021	-22,37
HS_S_23	Optional	666727	6247782	-23,98
HS_S_24	CPT	676401	6247736	-29,23
HS_S_25	Optional	678416	6247678	-30,11
HS_S_26	CPT	663578	6247360	-30,25
HS_S_27	CPT	673225	6247331	-26,09

MAV2023-050 Hesselø South

ID	Type	EUREF89 UTMX Z32 [m]	EUREF89 UTMY Z32 [m]	MSL EMODNET 2018
HS_S_28	CPT	670263	6246796	-23,14
HS_S_29	CPT	667362	6246251	-21,73
HS_S_30	CPT	659668	6246232	-22,1
HS_S_31	CPT	661896	6246044	-23,47
HS_S_32	SCPT + BH	663177	6245262	-28,02
HS_S_33	CPT	665192	6245204	-24,57
HS_S_34	Optional	659788	6244988	-21,42
HS_S_35	CPT	658200	6244785	-20,4
HS_S_36	CPT	661124	6244229	-21,06
HS_S_37	CPT	662562	6243295	-27,4
HS_S_38	CPT + BH	659183	6243037	-20,32
HS_S_39	CPT	656920	6242688	-18,52
HS_S_40	Optional	660434	6242250	-21,15

Appendix 8.6 Contextual information about samples

ETRS N	ETRS E	lab nr	Nr.	site	sample	Age BP		Correction		Elevation	sedi	Lab nr. for OxCal
6293731,25	674484,15	AAR-1576	1	Kattegat, corring, PC 10-07	Marine shells,	8840	75	400	8440	-53,20	3,22	R_Date("1", 8440, 75) {z=-53.20;color="blue"};
6242857,42	663248,37	AAR-1332	2	Kattegat, corring, K1	Marine shells,	6780	120	400	6380	-32,45	2,46	R_Date("2", 6380, 120){z=-32.45;color="blue"};
6236309,70	694830,10	AAR-1088	3	Kattegat, corring, Psh 2981	Marine shells, cardium shell	9030	100	400	8630	-27,11	3,11	R_Date("3", 8630, 100){z=-27.11;color="blue"};
6236309,70	694830,10	AAR-1086	4	Kattegat, corring, Psh 2981	Marine shells,	9340	160	400	8940	-24,80	0,80	R_Date("4", 8940, 160){z=-24.80;color="blue"};
6276885,82	672672,14	AAR-3042	5	Kattegat, corring, 572004	Marine shells, Mytilus Edulis	10120	75	400	9720	-25,30	3,50	R_Date("5", 9720, 75) {z=-25.30;color="blue"};
6276885,82	672672,14	AAR-3043	6	Kattegat, corring, 572004	Marine shells, Astarte Borealis	11930	100	400	11530	-39,47	5,57	R_Date("6", 11530, 100){z=-39.47;color="blue"};
6277650,91	673488,70	AAR-5058	7	Kattegat, corring, 572003	Marine shells, Portlandia Arctica	13070	100	400	12670	-39,00	5,70	R_Date("7", 12670, 100){z=-39.00;color="blue"};
6293731,25	674484,15	AAR-1575	8	Kattegat, corring, PC 10-07	Marine shells, Arctica islandica	11050	100	400	10650	-56,66	6,66	R_Date("8", 10650, 100){z=-56.66;color="blue"};
6232077,30	652994,77	St-2174	9	Kattegat, core B 504	Peat	9725	200	0	9725	-22,00	1,00	R_Date("9", 9725, 200){z=-22.00;color="green"};
6252192,83	700046,45	Ua-91	10	Kattegat, core 8533	Marine shells, Macoma calcarrea	12450	170	400	12050	-37,60	4,12	R_Date("10", 12050, 170){z=-37.60;color="blue"};
6252207,96	661067,02	AAR-3041	11	Kattegat, core 572002	Marine shells, Macoma baltica	9750	65	400	9350	-30,60	4,50	R_Date("11", 9350, 65){z=-30.60;color="blue"};
6260098,90	664351,86	AAR-4063	12	Kattegat, core no. 572012	Marine shells, Cerastoderma edule	9145	75	400	8745	-33,35	5,25	R_Date("12", 8745, 75){z=-33.35;color="blue"};
6260098,90	664351,86	AAR-4062	13	Kattegat, core no. 572012	Marine shells, Balanus crenatus, Cerastoderma edule	8520	55	400	8120	-28,70	0,60	R_Date("13", 8120, 55){z=-28.70;color="blue"};
6260144,24	663655,46	AAR-4061	14	Kattegat, core no. 212640	Marine shells, Cerastoderma edule, Macoma balthica	9235	55	400	8835	-30,20	2,30	R_Date("14", 8835, 55){z=-30.20;color="blue"};
6260458,27	653706,59	AAR-4537	16	Kattegat	Marine shells, Macoma baltica	9960	90	400	9560	-30,50	4,85	R_Date("16", 9560, 90){z=-30.50;color="blue"};
6236168,40	689796,93	AAR-5132	17	Kattegat	Marine shells, Portlandia arctica	13310	90	400	12910	-29,75	2,85	R_Date("17", 12910, 90){z=-29.75;color="blue"};
6235602,27	690657,11	AAR-5131	18	Kattegat	Marine shells, Macoma balthica	11040	60	400	10640	-29,03	2,50	R_Date("18", 10640, 60){z=-29.03;color="blue"};
6272681,59	660188,32	AAR-4527	19	Kattegat	Marine shells, Macoma baltica	13070	100	400	12670	-32,00	3,00	R_Date("19", 12640, 100){z=-32.0;color="blue"};

MAV2023-050 Hesselø South

ETRS N	ETRS E	lab_nr	Nr.	site	sample	Age BP		Correction		Elevation	sedi	Lab nr. for OxCal
6272681,59	660188,32	AAR-4527.1	21	Kattegat	Marine shells, Macoma baltica	13670	110	400	13270	-32,00	3,00	R_Date("21", 13270, 110){z=-32.00;color="blue"};
6260458,27	653706,59	AAR-4536	22	Kattegat	Marine shells, Mytilus edulis	9600	80	400	9200	-29,00	3,20	R_Date("22", 9200, 80){z=-29.00;color="blue"};
6260144,96	663662,35	AAR-4535	23	Kattegat, core no 572011	Marine shells, Mytilus edulis	10050	90	400	9650	-33,50	5,55	R_Date("23", 9650, 90){z=-33.50;color="blue"};
6252207,96	661067,02	AAR-4532	24	Kattegat, core no 572002	Marine shells, Mya truncata	8730	90	400	8330	-23,20	1,40	R_Date("24", 8330, 90){z=-23.20;color="blue"};
6261276,60	652969,19	AAR-4526	25	Kattegat, corring, 572017	Marine shells, Hiatella Arctica	14000	120	400	13600	-32,72	5,00	R_Date("25", 13600, 100){z=-32.72;color="blue"};
6252207,96	661067,02	AAR-4531	26	Kattegat, core no 572002	Marine shells, Corbula gibba	8340	80	400	7940	-22,80	1,00	R_Date("26", 7940, 80){z=-22.80;color="blue"};
6231348,30	683047,30	St-2171	27	Northern zealand	Peat	10820	200	0	10820	-26,70	1,70	R_Date("27", 10820, 200){z=-26.70;color="green"};
6267076,87	658476,72	AAR-4534	28	Kattegat, corring, 572009	Marine shells, Mytilus Edulis	10410	80	400	10010	-34,15	4,95	R_Date("28", 10010, 80){z=-34.15;color="blue"};
6267076,87	658476,72	AAR-4533	29	Kattegat, corring, 572009	Marine shells, Mytilus Edulis	10310	80	400	9910	-32,85	3,65	R_Date("29", 9910, 80){z=-32.85;color="blue"};
6267076,00	658476,72	K-6959	30	Kattegat, corring, 572009	Marine shells, Cerastoderma edule	9010	120	0	9022	-30,00	0,80	R_Date("30", 9022, 120){z=-30;color="blue"};
6261449,00	668702,00	Beta-585279	31	Hesselø, 5.2D, VC_15	Marine shells, Littorina	10060	30	400	9660	-33,90		R_Date("31", 9660, 30){z=-33.90;color="blue"};
6235402,00	692572,00	Beta-585280	32	Hesselø, 4.2D, GL03_14	Marine shells, Littorina	9790	30	400	9390	-30,00		R_Date("32", 9390, 30){z=-30.00;color="blue"};
6249604,00	673430,00	Beta-585281	33	Hesselø, 3.2D, GL06_05	Marine shells, Cerastoderma	9760	30	400	9360	-30,30		R_Date("33", 9360, 30){z=-30.30;color="blue"};
6236101,00	691845,00	Beta-585282	34	Hesselø, 3.3D, GL04_1A	Marine shells, Cerastoderma	9960	30	400	9560	-30,60		R_Date("34", 9560, 30){z=-30.60;color="blue"};
6274534,00	675206,00	Beta-585283	35	Hesselø, 2.2D, VC_02	Marine shells, Cerastoderma	7970	30	400	7570	-32,50		R_Date("35", 7570, 30){z=-32.50;color="blue"};
6256737,00	665264,00	Beta-585284	36	Hesselø, 2.3D, VC_23A	Plant material, twig	9020	30	400	8620	-30,60		R_Date("36", 8620, 30){z=-30.60;color="blue"};
6254849,00	663128,00	Beta-473575	38	MSM22	Marine shells	10260	30	400	9860	-35,60		R_Date("38", 9860, 30){z=-35.60;color="blue"};
6226633,32	650223,02	AAR-8841	39	core 258030	Marine shells	8275	65	400	7875	-28,30		R_Date("39", 7875, 65){z=-28.30;color="blue"};
6226633,32	650223,02	AAR-8840	40	core 258030	Marine shells	8410	80	400	8010	-30,60		R_Date("40", 8010, 80){z=-30.60;color="blue"};
6254943.10	646012,28	AAR-38173	41	Kattegat, KG 02 - P03 (B2) X8	Marine shells (sand with shell fragments)	4230	31	400	3830	-28,37	2,77	R_Date("41", 3830, 31){z=-28.37;color="blue"};

MAV2023-050 Hesselø South

<u>ETRS N</u>	<u>ETRS E</u>	<u>lab nr</u>	<u>Nr.</u>	<u>site</u>	<u>sample</u>	<u>Age BP</u>		<u>Correction</u>		<u>Elevation</u>	<u>sedi</u>	<u>Lab nr. for OxCal</u>
6251784.23	640259,76	AAR-38169	42	Kattegat, KG 07 - P01 (B1) X9	Marine shells (Clay with shell fragments)	4207	34	400	3807	-21,32	0,8	R_Date("42", 3807, 34){z=-21.32;color="blue"};
6251784.23	640259,76	AAR-38168	43	Kattegat, KG 07 - P01 (B2) X7	Marine shells (Clay with shell fragments)	2129	30	400	1729	-21,62	1,1	R_Date("43", 1729, 30){z=-21.62;color="blue"};
6249427.53	643640,64	AAR-38170	44	Kattegat, KG 12 - P03 (B2) X4	Marine shells (sand with shell fragments)	7538	44	400	7138	-21,09	2,66	R_Date("44", 7138, 44){z=-21.09;color="blue"};
6240084.01	634461,71	AAR-38172	46	Kattegat, KG 25 - P01 (B2) X10	Marine shells (sand with shell fragments)	4815	32	400	4415	-21,54	0,66	R_Date("45", 4415, 32){z=-21.54;color="blue"};
6240084,01	634461,71	AAR-38171	47	Kattegat, KG 25 - P01 (B2) X11	Hazelnut/nutshell (sand)	8871	45	0	8871	-21,54	0,66	R_Date("46", 8871, 45){z=-21.54;color="blue"};
6240084,01	634461,71	AAR-38166	48	Kattegat, KG 25 - P02 (B2) X5	Marine shells (organic material)	4545	42	400	4145	-22,29	1,39	R_Date("47", 4145, 42){z=-22.29;color="blue"};
6240084,01	634461,71	AAR-38167	49	Kattegat, KG 25 - P02 (B2) X6	Wood (organic material)	9148	53	0	9148	-22,29	1,39	R_Date("48", 9148, 53){z=-22.29;color="blue"};
6252621,00	670303,40	AAR-38165	51	Hesselø, HS 06 - P2 (B3) X1	Cardium shell (clay)	9057	48	400	8657	-29,87	4,99	R_Date("49", 8657, 48){z=-29.87;color="blue"};
6250566,90	664070,40	AAR-38163	52	Hesselø, HS 11 - P2 (B1) X3	Marine shells (sand with shell fragments)	9101	42	400	8701	-32,69	4,38	R_Date("50", 8701, 42){z=-32.59;color="blue"};
6250566,90	664070,40	AAR-38164	53	Hesselø, HS 11 - P2 (B1) X2	Wood (sand)	8861	50	0	8861	-32,69	4,38	R_Date("51", 8861, 50){z=-32.69;color="blue"};